Ultraviolet-Visible (UV-Vis) Spectroscopy

11

Charlotte Vogt ⓘ, Caterina Suzanna Wondergem ⓘ, and
Bert M. Weckhuysen ⓘ

Contents

Abstract

Ultraviolet-Visible (UV-Vis) spectroscopy is a versatile and powerful analytical method, which allows to

investigate a wide variety of catalysts in both the liquid-phase and solid-state and their interfaces at elevated temperatures and pressures. In the case of solid catalysts, they can be studied in the form of powders (e.g., in diffuse reflectance mode) and as thin wafers (in transmission mode), and when combined with a microscope even in the form of catalyst bodies (e.g., extrudates) and single crystals. In the past two decades, UV-Vis spectroscopy has been increasingly used under *in situ* and *operando* conditions to shed light on/gain insight in the working principles of heterogeneous catalysts, homogeneous catalysts, electrocatalysts, as well as photocatalysts. One of the advantages of this method is that it can simultaneously measure, e.g., the electronic transitions of organic molecules (mainly via their $n \rightarrow \pi^*$ and $\pi \rightarrow \pi^*$ transitions) and transition metal oxides or ions (via their d-d and charge transfer transitions). Unfortunately, absorption bands in the UV-Vis range are often broad and overlapping and hence their interpretations are not always trivial. Advanced theoretical calculations are required to provide a proper foundation of their interpretation, while, e.g., chemometrics can help prevent biased analysis when many (time-resolved) spectra are collected. Finally, UV-Vis spectroscopy is often combined with other analytical methods to provide complementary information. Examples include X-ray absorption spectroscopy and diffraction, next to vibrational spectroscopy (i.e., infrared and Raman) and magnetic resonance (i.e., electron spin resonance and nuclear magnetic resonance) methods. The above-described scientific and instrumental developments will be illustrated by using a selection of showcase examples, covering the different areas of catalysis. The chapter concludes with some main observations as well as some future developments on what might become possible in the not-too-distant future.

C. Vogt
Schulich Faculty of Chemistry, Technion, Israel Institute of Technology, Haifa, Israel
e-mail: c.vogt@technion.ac.il

C. S. Wondergem
Research Center for Materials Science, Graduate School of Science, Nagoya University, Nagoya, Japan
e-mail: cswondergem@chem.nagoya-u.ac.jp

B. M. Weckhuysen (✉)
Inorganic Chemistry and Catalysis, Debye Institute for Nanomaterials Science, Utrecht University, CG Utrecht, The Netherlands
e-mail: b.m.weckhuysen@uu.nl

11.1 Basic Principles of Ultraviolet-Visible Spectroscopy

Ultraviolet-Visible spectroscopy makes use of radiation in the Ultraviolet (UV) and Visible (Vis) radiation regions of the electromagnetic spectrum from approximately 200–800 nm $(50,000–12,500 \text{ cm}^{-1})$ [1]. Often the spectroscopic method extends into the near-infrared (NIR) region and is then referred to as UV-Vis-NIR spectroscopy, with a spectral range up to, e.g., 2000 nm (i.e., down to 5000 cm^{-1}). The UV range constitutes the first 200–400 nm of the spectrum, followed by the Vis region (400–800 nm) and finally the NIR region (>800 nm). In UV-Vis-NIR spectroscopy, the interaction of UV, Vis, and NIR radiation photons with the sample is measured. Since this is partly the same region as where human eyes detect color, the absorption, scattering, or reflectance of UV-Vis-NIR radiation and thus the suitability of the characterization technique for a particular sample can (roughly) be qualitatively predicted by its color. Completely black samples, as is the case for solid catalysts containing coke deposits, are often not suitable for UV-Vis-NIR spectroscopy as they may absorb all the incident photons, whereas completely white or transparent samples are not likely to be suitable either, as they may reflect, scatter, or transmit (respectively) all incident radiation depending on, e.g., the dimensions of the grains or crystals constituting the catalyst material. The latter can be the case when investigating (high-valency) transition metal oxides (e.g., Re_2O_7) supported on a silica support. Samples of which color changes occur during reaction (e.g., $CrO_3 \rightarrow Cr_2O_3$) or those that are vibrantly colored (e.g., a solid containing an organic dye molecule as can be formed/synthesized/produced within the channels of a zeolite-based catalyst) are generally particularly suitable for UV-Vis-NIR spectroscopy.

UV-Vis-NIR spectroscopy is often called electronic spectroscopy because electrons are transferred from low-energy into high-energy atomic or molecular orbitals when the material is irradiated with electromagnetic radiation [2]. The $\sigma \rightarrow \sigma*$ transitions in organic molecules (e.g., originating from a C-H or C-C chromophore) are generally high-energy transitions with corresponding short wavelength (i.e., λ often below 200 nm). These transitions are generally not observed with UV-Vis-NIR spectroscopy unless vacuum is applied and/or synchrotron-based UV-radiation (and related detection) is employed because such transitions will also be probed in the molecules that make up air (e.g., O_2), and vacuum or higher photon flux from synchrotron radiation are ways to eliminate this issue. A similar situation exists for $n \rightarrow \sigma*$ transitions (e.g., NH_2 chromophore), which occur at ~150–250 nm. On the other hand, $n \rightarrow \pi*$ (e.g., C=O chromophore) and $\pi \rightarrow \pi*$ (e.g., C=C chromophore) transitions occur with incident radiation of approximately 200–700 nm and show weak and intense absorption responses, respectively. As such, many organic molecules containing (conjugated) π systems, as is the case for aromatic compounds, as well as metal-organic species and transition metal complexes (which possess characteristic d-d transitions or charge transfer (CT)), are species excellent for detection with UV-Vis-NIR spectroscopy. The NIR addition to UV-Vis spectrometers is especially useful as it allows to detect the combination and overtone bands of characteristic vibrational bands of, e.g., adsorbed organic molecules (e.g., aromatics) or the terminal groups of metal oxides (e.g., silanol groups of a SiO_2 support). Furthermore, the more delocalized the electrons are in a system (i.e., the more conjugated the bonds of a molecule are in, e.g., an aromatic species), the lower the energy required to excite an electron from its ground state. Consequently, the absorption peak for similar molecules with increasing degree of conjugation will be found at increasingly higher wavelengths in the UV-Vis absorption spectrum. Additional background on the principles, theory, and applications of UV-Vis-NIR spectroscopy in the field of catalysis can be found in several book chapters and review articles.

As becomes clear from Table 11.1, the application of UV-Vis-NIR spectroscopy in catalysis is particularly relevant to study transition metal ion (TMI) centers (in particular 3d-ions), rare earth metal ions (especially lanthanides), adsorbed molecules, molecular ions and (organic) radicals, and catalyst supports (which can be amorphous metal oxides with a high surface area or porous crystalline materials, such as zeolites, metal organic frameworks (MOFs) and mesoporous materials). In the case of 3d-ions, detailed UV-Vis-NIR characterization studies can be performed on the low-valent transition metal cations (i.e., Cu^{2+}, Cr^{3+}, Co^{2+}, and Ni^{2+}) revealing their coordination environment in the

Table 11.1 Overview of the possible transitions that can be probed with UV-Vis-NIR spectroscopy and are relevant to the characterization of catalysts

Species	Relevant transitions
Transition metal ion	d-d transitions, metal-to-ligand charge transfer (MLCT) transitions, ligand-to-metal charge transfer (LMCT) transitions
Rare earth ions	f-f and f-d transitions
Molecules, radicals, molecular ions	$n \rightarrow \pi*$ and $\pi \rightarrow \pi*$ transitions
Supports (oxide)	Band gap, impurities, defects
Supports, inorganic and organic species	Overtone and combination bands of vibrations in the infrared region
Multinuclear mixed-valence species	Intervalence charge transfer (IVCT)

presence and absence of reactants, while for high-valent transition metal anions (i.e., Cr^{6+}, V^{5+}, Mo^{6+}, and Re^{7+}) the redox behavior and nuclearity (e.g., chromate, dichromate, and polychromate) can be investigated as a function of, e.g., support oxide and reduction conditions. Examples of the former can be found in the work of the groups of, e.g., Schoonheydt [3], Che [4], Zecchina [5], and Wichterlova [6], while the latter has been performed by a.o. the groups of Wachs [7], and Bell/Iglesia [8]. The earlier works of Che, Wichterlova, and Schoonheydt on first row transition metal ions, such as $Cu^{2+/+}$ and $N^{i2+/+}$, already illustrated the strong complementarity of UV-Vis-NIR spectroscopy with another powerful analytical method, namely, Electron Spin Resonance (ESR) which also measures ground state properties of transition metal ions (e.g., V^{4+} (d^1) and Cu^{2+} (d^9). This has been nicely summarized by Sojka et al. [9].

Two theories that are highly relevant to explain the effects observable by UV-Vis-NIR spectroscopy are Crystal Field Theory (CFT) and Molecular Orbital Theory (MOT) [10]. CFT describes the breaking of degeneracies of electron orbital states, while MOT uses quantum mechanics to describe the electronic structure of molecules. These theories describe the origins and the consequences of interactions of the surroundings on the orbital energy levels of transition metal ions and conjugated π-system, among others. Such interactions are considered electronic even if there is no net charge, as lone pairs of electrons are interchanged. When considering a transition metal ion, molecular ion, or radical, and its interaction with an adsorbate, such adsorbates are considered point negative charges surrounding the ionic radius of the ion or radical under consideration. In this case the corresponding energy is the crystal field potential (Eq. 11.1), where R_j is the distance of the ion-adsorbate j, r_i is the distance between the ion-electron i, and n is the number of adsorbates.

$$V(r_i) = \sum_{j=1}^{n} \frac{e^2}{|R_j - r_i|} \qquad (11.1)$$

For m electrons the crystal field potential is given as Eq. 11.2:

$$V_{CF} = \sum_{i=1}^{m} V(r_i) \qquad (11.2)$$

The crystal field potential causes destabilization of d-orbitals (to differing extents, based on their orientation). Depending on the applied crystal field geometry (e.g., octahedral coordination) and the (non-)axial nature of the orbitals, splitting of d-orbital energies into relatively lower and higher energies can occur. This separation is then given as Δ_0 and suggests that the electrons that occupy the

d-orbitals can rearrange. An electron can be excited from the low energy d-orbitals to the high energy ones by absorption of a photon with the corresponding energy. This energy is represented by $\Delta E = h\nu = \Delta_0$. Such rearrangements form the basis of d-d spectra (crystal field spectra), and a large part of electronic absorption spectra. However, electronic absorption spectra also include charge transfer complexes, and interelectronic transitions. Charge transfer complexes involve the association of two or more molecules in which a fraction of electronic charge is transferred between the molecular entities. The resulting electrostatic attraction provides a stabilizing force for the molecular complex.

The combination of CFT and MOT led to the more realistic and complex ligand field theory (LFT), which can give insight into the chemical bonding of (supported) transition metal ion complexes. A recent literature example can be found in the elucidation of the redox properties of Mn-promoted sulfated ZrO_2, a highly active alkane isomerization catalyst, by in situ UV-Vis spectroscopy and CFT [11]. More specifically, a cluster model that considers the Mn center as a complex with the adjacent ions of the lattice as ligands was developed and used to determine the Mn^{3+}/Mn^{4+} ratio in the catalyst based on temperature-dependent UV-Vis spectroscopic data. The combination of such theories with density functional theory (DFT) has allowed for accurate modeling of UV-Vis-NIR spectra of model complexes, a tool now often used in literature to build, e.g., libraries providing the ability to relate specific species to convoluted spectra or real system, thereby increasingly approaching realistic reaction environments (i.e., the operando approach). This aspect will be later on illustrated with some showcases in the field of zeolite-based catalysis and olefin polymerization catalysis.

There are several excellent reference works describing the principles and applications of UV-Vis-NIR spectroscopy in the broad field of catalysis. To the best of our knowledge, the last review paper has been written by Jentoft in 2012, which appeared in a textbook edited by Che and Védrine [12], but also noteworthy are the 2010 Chemical Society Reviews paper by Schoonheydt [13], the 2009 Advances in Catalysis paper by Jentoft [14] and the older reviews by Schoonheydt [15], Kellerman [16], Klier [17], as well as the textbook of Kortüm [18]. Our own review articles date back to one 1999 Catalysis Today paper [19] and two book chapters in 2000 [20] and 2004 [21], in which the state-of-the-art of in situ and operando UV-Vis-NIR diffuse reflectance spectroscopy of solid catalysts has been summarized. Hence, this chapter approximately summarizes the tremendous progress made in this field of research the past 20 years. In this time, the instrumental capabilities have increased dramatically, offering more possibilities currently than we could have imagined 20 years ago. Among these new possibilities is the branching out of UV-VIS-NIR spectroscopy to other application

domains, including photocatalysis and electrocatalysis. The search for complementarity with other analytical methods is now well-established as no single technique can provide the ultimate answer to a fundamental catalytic problem. Furthermore, UV-Vis-NIR spectroscopy is increasingly used under relevant reaction conditions, including the verification that the measurement cell indeed performs (to a certain degree) as a catalytic reactor (i.e., the *operando* measurement approach [22]).

11.2 The Spectrometer and Related Accessories

11.2.1 The UV-Vis Spectrometer

A UV-Vis spectrometer can be a relatively inexpensive piece of laboratory equipment and generally has the following basic components; a source of UV-Vis radiation, a monochromator which ensures the correct wavelength of radiation illuminates the sample, a sample holder, and a detector. In a typical spectrometer for liquid-phase measurements, these components are placed on a single axis, as shown in Fig. 11.1. The monochromator gradually changes its energy

along a given set of energies in the region of interest, and the photons that reach the detector are counted. Because the amount of photons output by the source (I_0) is known, the transmission of the sample can be calculated (the measured intensity through the sample (I) divided by the intensity of the source, I/I_0). In a classical UV-Vis spectroscopy measurement, often a cuvette with a precise path length is filled with the sample, which can be a solution containing solvent, reactant, and a homogeneous catalyst. The amount of radiation that is absorbed by the sample depends on its concentration, the path length of the radiation through the cuvette, and how much radiation the sample absorbs at a certain wavelength. The absorbance can be calculated by taking the natural logarithm of the transmittance (T) (Eq. 11.3), and this is in turn related to the concentration of the sample via Lambert-Beer's law (Eq. 11.4).

$$A = -\log 10(T) \tag{11.3}$$

$$A = \varepsilon l c \tag{11.4}$$

where A is absorbance (unitless); ε is the molar absorption coefficient, or molar absorption constant of the sample for a

Fig. 11.1 (**a**) Schematic representation of the basic components of a UV-Vis spectrometer, including a proper radiation source, a wavelength selector, sample holder, and detector; and (**b**) The difference between specular reflected radiation (radiation reflected in a mirror-like fashion, at a definite angle) and diffuse reflected radiation (the reflection of radiation from a surface such that an incident ray is reflected at many angles), which forms the basis of UV-Vis spectroscopy when working with, solid catalysts
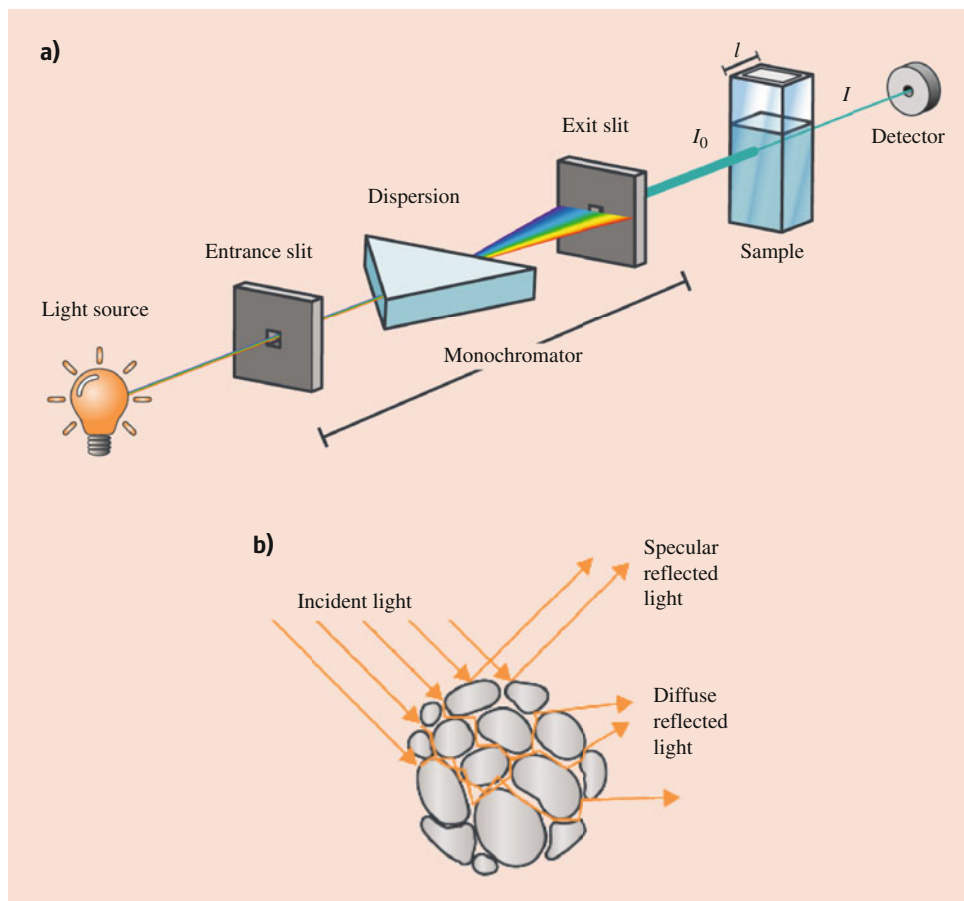
certain wavelength ($L \cdot \text{mol}^{-1} \cdot \text{cm}^{-1}$); l is path length (cm) through the cuvette; and c is the concentration of the sample ($\text{mol} \cdot \text{L}^{-1}$). In other words, for simple solution-based experiments quantitative UV-Vis experiments can be performed, allowing to elucidate the change of a coordination complex of a transition metal ion as a function of reaction time.

UV-Vis spectroscopy is a fast and simple method with which one can determine the concentration of the sample or molecule, being it either a reactant, reaction, intermediate, or reaction product under investigation. It is a versatile method that can be applied to gases, liquids, and solids. UV-Vis spectroscopy is extremely sensitive to concentrations and is also a noninvasive technique, which make it possible to perform *in situ* measurements for, e.g., chemical reactor control. Downsides of UV-Vis spectroscopy are the fact that the technique is diffraction-limited and hence the spatial resolution is limited to ~0.5 μm when combined with a microscope, and that the signals that are obtained are generally broad and convoluted, meaning that several components have overlapping features. Furthermore, for characterization of solid catalysts, it is often difficult to obtain UV-Vis transparent samples (i.e., thin-films of powdered samples are difficult to obtain), which limits the application of, e.g., transmission UV-Vis spectroscopy. There are only a few examples of zeolites being pressed into self-supported catalyst wafers allowing for the UV-Vis transmission study of solid catalysts (in use) [23–25]. The limiting factor is that much of the radiation does not reach the detector due to scattering. To that end, diffuse reflectance spectroscopy (DRS) can be applied, where the radiation that is diffusely reflected off the sample is collected by convergent mirrors or an integration sphere. In what follows, we will discuss the different modes of measuring UV-Vis-NIR spectroscopy, including fiber optics UV-Vis spectroscopy, but we refer to the earlier cited book chapters and review articles for a more comprehensive overview of the different cell designs and measurement options available [12–21].

11.2.2 Sample Preparation, Mode of Measuring, and Catalytic Reactors

The typical undergraduate degree laboratory introduction to UV-Vis spectroscopy is to measure calibration lines in a cuvette for a solution with a specific concentration of an analyte [1, 2]. While surely interesting as an analytical technique in that sense, the cuvette has little relevance for the application of UV-Vis spectroscopy for studying chemical reactions taking place in the presence of, e.g., a homogeneous or heterogeneous catalyst. For most catalytic applications, requirements of an experimental setup for *in situ* or *operando* UV-Vis spectroscopy are – next to a suitable spectrometer – a methodology apt to measure with sufficient signal-to-noise

ratio and operable at reaction conditions of elevated temperatures and/or pressures. By doing so, a setup is used that mimics to a certain extent the reactor type (e.g., plug flow) of the catalytic reactor when there is no spectroscopy involved. The latter aspect is often evaluated by attaching a residual gas analysis device to the *operando* setup, such as a mass spectrometer (MS) or a gas chromatograph (GC), in order to ensure that product formation is as expected, and true structure-reactivity correlations can be made [22]. The *operando* UV-Vis spectroscopy approach (employing online GC analysis) in the field of heterogeneous catalysis was already practiced at the end of the 1990s [26], and at the start of the 2000s [27, 28], although it was not yet coined that way, and *operando* UV-Vis spectroscopy formally entered the scientific literature in 2003 when two combined setups (UV-Vis/Raman spectroscopy [29] and ESR/UV-Vis spectroscopy [30]) were first discussed at the first Congress on Operando Spectroscopy (Lunteren, the Netherlands).

As mentioned above, it can be difficult to prepare heterogenous catalytic samples in particular, samples that are UV-Vis transparent, and while it has been proven to be advantageous to measure in transmission in some cases [31], more often than not high absorption and scattering limit the application of transmission-mode UV-Vis spectroscopy for heterogeneous catalysis. As such, there are three main modes of operation for UV-Vis spectroscopy that have become highly relevant to catalysis research.

1. Diffuse reflectance UV-Vis (DRS, or DR-UV-VIS) spectroscopy, either by use of a Praying Mantis™-type accessory or (to a lesser extent) by use of a classical diffuse reflectance integrating sphere, which is typically coated with materials that reflect more than 95–99% of radiation in the relevant spectral region
2. UV-Vis spectroscopy by fiber optics (a variation of diffusion and specular reflectance), and
3. UV-Vis micro-spectroscopy (a variation of diffusion and specular reflectance, or transmission depending on the mode of operation).

Transmission Spectroscopy
The application of transmission UV-Vis spectroscopy is the preferred mode of measurement, as this is the simplest mode, requiring the least amount of additional contributing factors. For typical homogeneous catalytic experiments, provided that the solution has sufficient transmission of UV-Vis radiation, the setup need not be different from that described in Fig. 11.1; a simple cuvette will then often suffice, although this cuvette can be adapted to make it possible to apply both temperature and pressure. To perform, e.g. (homogeneous) electrocatalytic experiments, one can include a working electrode, counter electrode, and reference electrode in the cuvette provided they are small enough and are not in the optical path of the

UV-Vis beam. For these types of reactions, standard spectroscopic equipment can generally be used. Performing heterogeneous electrocatalytic experiments in transmission mode should in principle be possible if the sample can be prepared as a thin-film, while still providing sufficient transmission, although it might be more relevant to measure such heterogeneous systems (including photocatalysis) using the experimental methodologies discussed below.

Nevertheless, there are only limited examples of heterogeneous catalysts successfully measured in transmission mode (e.g., zeolites [9–11]), as these samples have to be sufficiently thin and non-absorbing to allow such measurements. A self-supported catalyst wafer of a support material or catalyst can sometimes fulfill these requirements. These

wafers are prepared by grinding and sieving catalyst or support particles (optional), and later applying an appropriate amount of pressure in a pellet press with a dye. Around a few tons of pressure is typically sufficient to create appropriate wafers. Care should be taken not to apply too much pressure, as the material will become very brittle and crystal structures may be damaged. In addition, a certain degree of gaseous transmission is required for *in situ* measurements.

As a showcase, Fig. 11.2a shows a self-supported catalyst wafer of H-SAPO-34, used as a catalyst in the Methanol-to-Olefins (MTO) reaction, of 16 mm diameter and around 0.1 mm thickness, weighing 5–7 mg, by using a Laboratory Pellet Press and around 4 tons of pressure under vacuum [32]. These prepared wafers can be placed in commercial

Fig. 11.2 (**a**) Picture of different catalyst wafers for measuring transmission UV-Vis spectroscopy under *operando* conditions; (**b**) An example of a spectroscopic setup that can be used for *operando* UV-Vis spectroscopy studies of self-supported catalyst wafers in transmission (or reflection) mode, as used for, e.g., the methanol-to-olefins (MTO) reaction over zeolite-based catalysts; and (**c**) Picture of the particular cell design for transmission *operando* UV-Vis spectroscopy measurements. (Reproduced from [32]; with permission from Wiley-VCH)
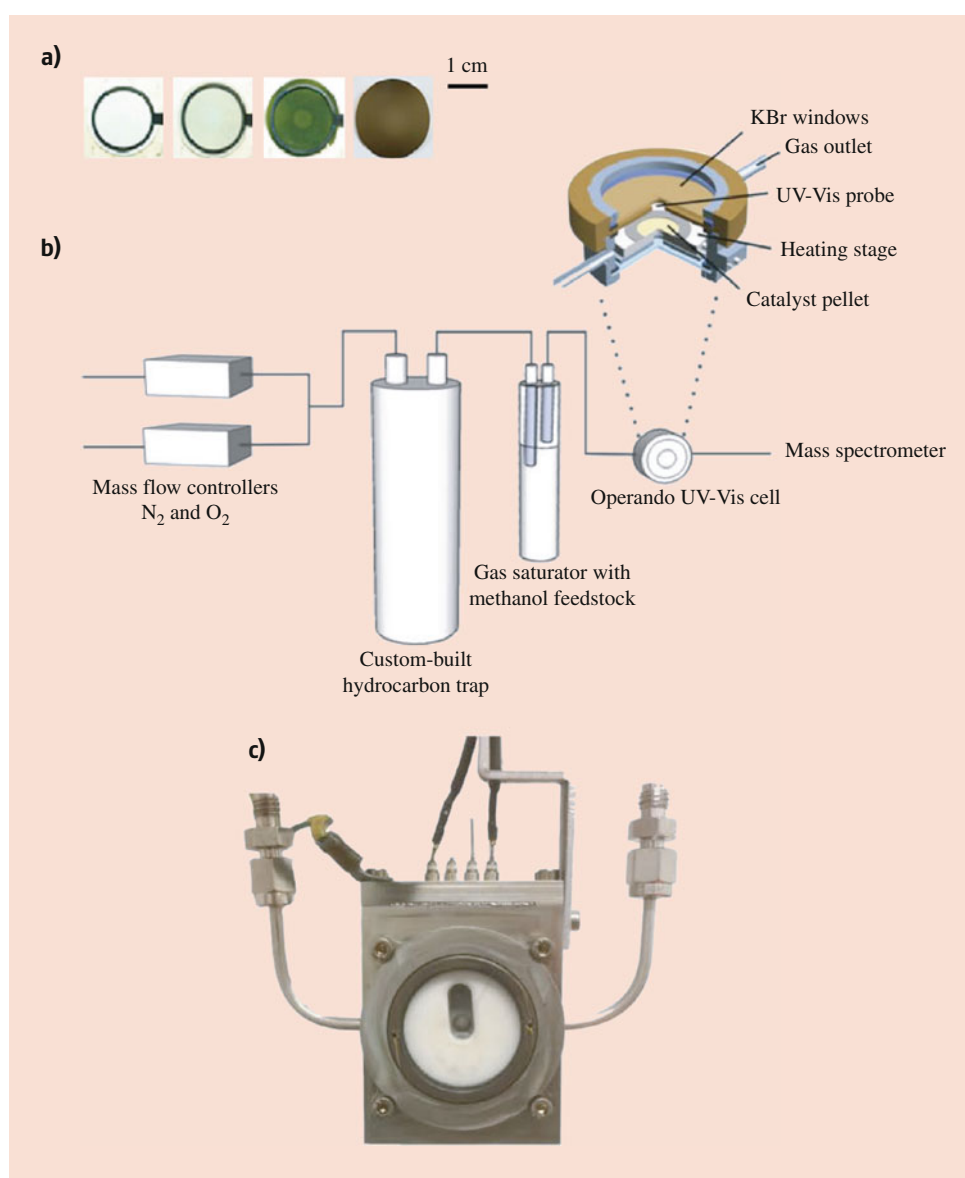
transmission cells with appropriate windows, such as those designed by Linkam (Fig. 11.2b, c). These cells contain a heating stage, liquid cooling, and gas connections, so that a catalytic experiment may be performed in the gas-solid or liquid-solid range. Depending on the modes of operation, the specific requirements of the catalytic reaction and the sample, and the potential coupling with other spectroscopic techniques, one may choose to design spectroscopic cells specifically for the experiment in mind. One of the important aspects to verify is that the dead volume of the cell is low to avoid contributions of the gas-phase, as well as to ensure a timely response on the online GC or MS device by decreasing the length of the gas lines between cell and GC or MS device when structure-performance relationships have to be established. This can be done by performing a pulse experiment and following a time-on-stream GC or MS profile. The *operando* transmission UV-Vis spectroscopy setup with online MS in Fig. 11.2 has been used to investigate the effect of different types of impurities (i.e., feed and internal impurities) on the hydrocarbon pool species [32]. It was found that feedstock impurities strongly influence the location of coke deposits, whereas organic impurities retained after regeneration function as "seeds" for coke formation.

Diffuse Reflectance Spectroscopy

Diffuse reflectance measurement cells for performing *in situ* or *operando* UV-Vis spectroscopy measurements, making use of the Praying Mantis™-type accessories as schematically shown in Fig. 11.3a, are now widely available for powdered samples, offering a plug-flow type reactor (Fig. 11.3b). These cells make use of convergent mirrors to collect diffuse-reflected radiation off of the loaded catalyst powder in the reactor cell, allowing it to be studied at elevated temperatures and under gaseous atmosphere, which fulfills all of the requirements listed above. This Praying Mantis™ setup was also the first one used for performing *operando* UV-Vis-NIR spectroscopy of supported metal oxide catalysts [26, 27].

A classical integration sphere is shown in Fig. 11.3c and is usually acquired as an accessory with a UV-Vis-NIR spectrometer when someone wants to conduct diffuse reflectance spectroscopy (DRS) measurements of powdered materials. This cell can then be used, shown in Fig. 11.3d, to measure solid catalysts under hydrated/dehydrated or oxidized/reduced conditions at room temperature [19–21]. However, the classical integration sphere is more problematic to use when performing *in situ* or *operando* measurements of catalysts. Due to this, there are no commercial cells available. Nevertheless, *in situ* cells have been developed in academic labs, as the one shown in Fig. 11.3e [33]. The sample is then positioned outside the integration sphere in a quartz container surrounded by a heating mantle. This cell can be operated at

elevated temperatures and pressures (e.g., temperatures <200 °C and <10 bar), but it should be clear that for many heterogeneous catalytic reactions this cell design becomes less applicable. It is important to recall that the function of the diffuse reflectance accessory is to direct the radiation from the source onto the sample, and subsequently to collect (as much as possible of) the reflected diffuse radiation and guide this reflected radiation back to the detector.

UV-Vis diffuse reflectance spectroscopy can be a quantitative technique, following the model of diffuse-reflected radiation by Kubelka and Munk. The propagation of radiation through inhomogeneous media (i.e., catalyst samples) differs significantly from the propagation of radiation in a homogeneous material, as radiation can also scatter at specific points in its path. Additional difficulty arises here for the study of solid catalysts because catalyst particles can be at the order of magnitude of the wavelength of the radiation used to irradiate the sample (e.g., ~0.1–1 µm). This complicates distinguishing between certain different interaction phenomena of the UV-Vis radiation with the catalyst's particles, such as reflection, refraction, and diffraction. Here we refer the reader to the textbook of Kortüm for more background [16]. Figure 11.1b includes the difference between specular reflection and diffuse reflectance. The latter forms the basis of the so-called Kubelka-Munk-Schuster (KMS) theory, often short noted as Kubelka-Munk (KM) theory, which explains in a quantitative manner how diffuse reflected radiation interacts with a powdered sample. More specifically, the KM model has a particularly simple solution in the case of semi-infinite samples. All the geometric peculiarities of the inhomogeneous sample are condensed into a single parameter, the scattering coefficient s. The diffuse reflectance R_∞ (the IUPAC recommendation is the use of ρ to describe the reflection, but for simplicity here we use R) is then given as:

$$R_\infty = 1 + \frac{k}{s} - \sqrt{\frac{k}{s}\left(2 + \frac{k}{s}\right)} \tag{11.5}$$

where k is the absorption coefficient of the sample ($k = 4^K/\lambda$, with K the extinction coefficient). The KM transformation (Eq. 11.6) yields a value that is approximately proportional to the absorption coefficient and can hence be used to determine values of the concentration of the analyte to be measured.

$$\frac{k}{s} = F(R_\infty) = \left(\frac{(1 - R_\infty)^2}{2R_\infty}\right) \tag{11.6}$$

In the limiting cases, indeed this expression yields correct values. That is, for a non-absorbing sample ($K \rightarrow 0$), all radiation should be reflected and indeed, $R_\infty \rightarrow 1$, whereas
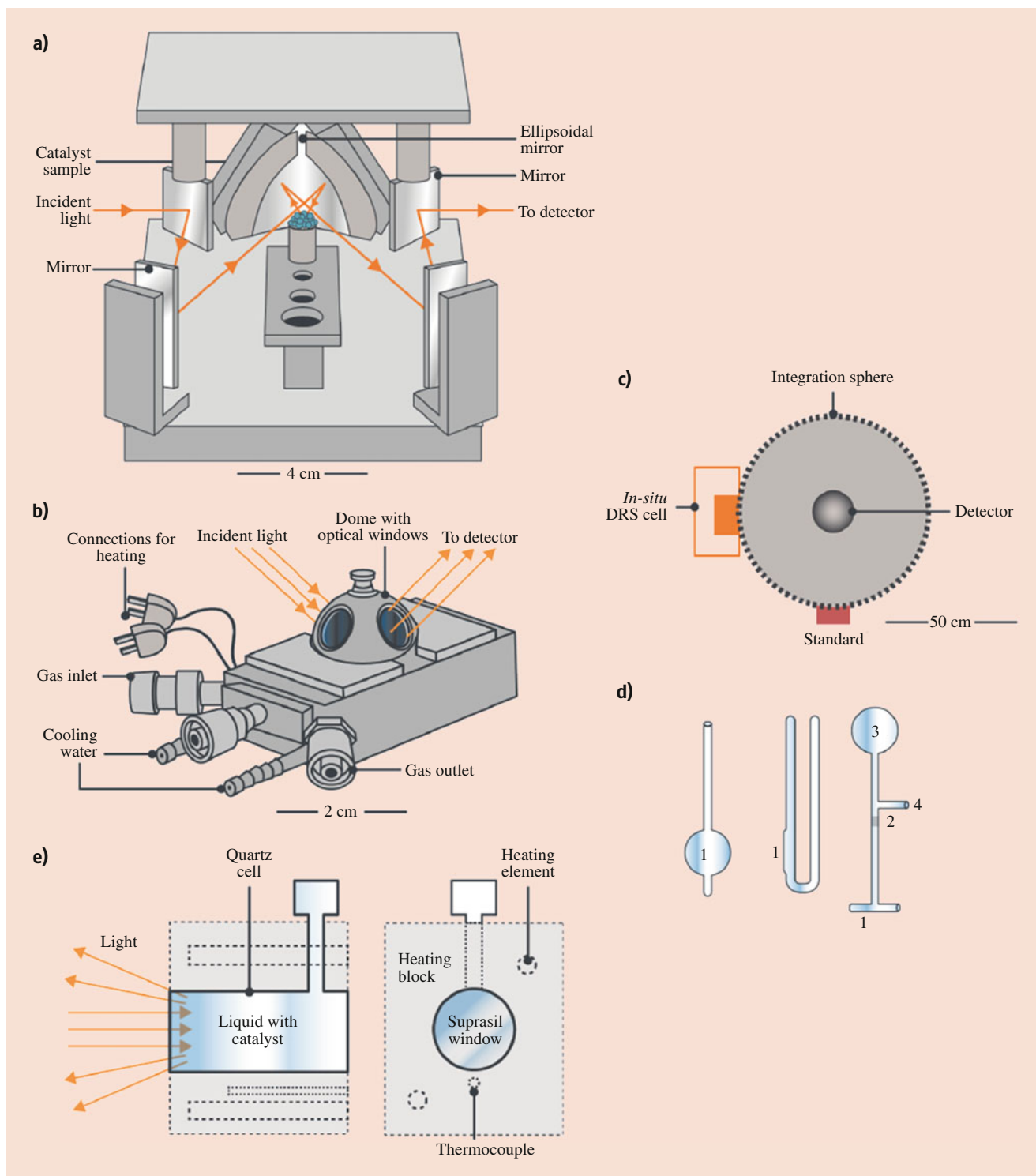
Fig. 11.3 Schemes of different *ex situ & in situ* and *operando* diffuse reflection spectroscopy methodologies and related measurement cells. (**a**) Schematic overview of a Praying Mantis™ accessory that can be used to focus UV-Vis radiation onto a powdered catalyst sample and collect the diffuse reflectance component and guide it to the detector; (**b**) An *in situ* cell that can be used in combination with a Praying Mantis™ in order to focus radiation onto powdered samples in a plug-flow-type configuration, while reacting with gases at elevated temperatures and pressures; (**c**) An integration sphere coated with, e.g., Halon white, MgO or BaSO4 can be used to perform *in situ* experiments, within a limited frame of temperature; (**d**)

Different UV-Vis reactors that can be used for UV-Vis spectroscopy studies; left and middle, quartz window (indicated by the number 1) cells, which can be filled with catalyst powder, and suitable for *ex situ* measurements of dehydrated/hydrated or oxidized/reduced materials; while the right sample holder can be used to heat a sample under vacuum conditions in the ball (indicated with number 3); number 2 and 4 indicate, respectively, a frit; and 4 the exit toward the vacuum pump; and (**e**) Schematic overview (side view, left; front view, right) of an *in situ* cell which was designed to measure solids operating in liquid-phase, which can operate at max 150 °C due to limitations of the integration sphere of a diffuse reflectance spectrometer

for a sample that does not scatter ($S \rightarrow 0$), no radiation should be reflected and indeed $R_\infty \rightarrow 0$.

Care must be taken since this approximation is only valid under the following conditions:

1. Diffuse, monochromatic irradiation of the sample occurs.
2. There is isotropic radiation scattering (the scatterer is small relative to the wavelength of the radiation and even in all directions). For this point it is particularly useful to (grind and) sieve catalyst fractions and use particles of a similar sieve fraction. Although this should be standard practice in catalyst sample preparation, for these types of experiments it becomes extra important.
3. Infinite layer thickness. This criterion can often be met by a (densely packed) sample thickness of 5 mm, although for some supports thicker layers may be required.
4. Sufficiently low concentration of absorbing centers.
5. Uniform distribution of adsorbing centers.
6. Absence of fluorescence.

Fiber Optics Spectroscopy

In the past two decades we have seen a rapidly expanding availability of suitable fiber optics to perform UV-Vis spectroscopy of catalytic processes. Fibers of ~5–10 mm in diameter, which contain in their tip both access to the source and the detector of a spectrometer work in reflection or backscattering mode, as shown in Fig. 11.4a. Such fibers are available for dipped-probe experiments (where the probe is submerged in a liquid) relevant to experiments in the liquid-phase, as well as non-dipped probes (i.e., which are placed either outside of the reactor environment measuring through a UV-Vis transparent window, or are placed inside the reactor with gaseous environment). These probes typically have path lengths of ~2–50 mm, allowing choice of probe functionality, and placement options to a wide range of experimental designs for *in situ* or *operando* catalytic experiments, relevant to both homogeneous and heterogeneous (electro)catalysis.

Fiber optic UV-Vis spectroscopy technically also operates under diffuse reflecting conditions, yet their mode of operation is significantly different from the classical integration spheres and other well-known examples of UV-Vis diffuse reflectance spectroscopy experimentation modes. Optical fibers redirect the beam from the UV-Vis source to the detector unit flexibly, through fibers that are usually made of silica. The radiation in the fibers is directed via total internal reflection to the head where the radiation can interact with the sample and the reflection returns to the detector via a different fiber. These fibers can either be in the same head, or in two different ones.

The cells described under the UV-Vis diffuse reflectance spectroscopy subsection already mimic catalytic reactions to a certain extent, and the gas outlets of such cells can be plugged onto gas analysis systems like a GC or a MS to analyze the reactants and reaction products. In such a way, *operando* mode of operation can be [easily] verified. However, one of the major advantages of UV-Vis spectroscopy is that it is possible to use fiber optics to connect to a reactor.

As UV-Vis spectroscopy is a truly noninvasive technique, a 5 mm hole in a real catalytic reactor can be used to insert the probe to noninvasively follow reactants and products, while the solid catalyst is at work. The first fiber optics *operando* UV-Vis spectroscopy experiment was performed in 2001 which probed Cr/Al_2O_3 catalysts during the propane dehydrogenation reaction [34]. Since then, several different *operando* UV-Vis spectroscopy designs have been realized including one that comes truly close to a real industrial reactor system is shown in Fig. 11.4b, c. Here, optical fiber UV-Vis and Raman probes are placed at different parts of a large propane dehydrogenation pilot reactor to monitor Cr-species as well as hydrocarbon deposits in catalyst extrudates as a function of the path length of the reactor. Sattler et al. demonstrated such an approach is practically feasible for a 1-m long reactor setup [35, 36]. The downsides of using such optical probes include lower radiation efficiency, and hence a lower signal (typically around 10% compared to a normal UV-Vis spectrometer).
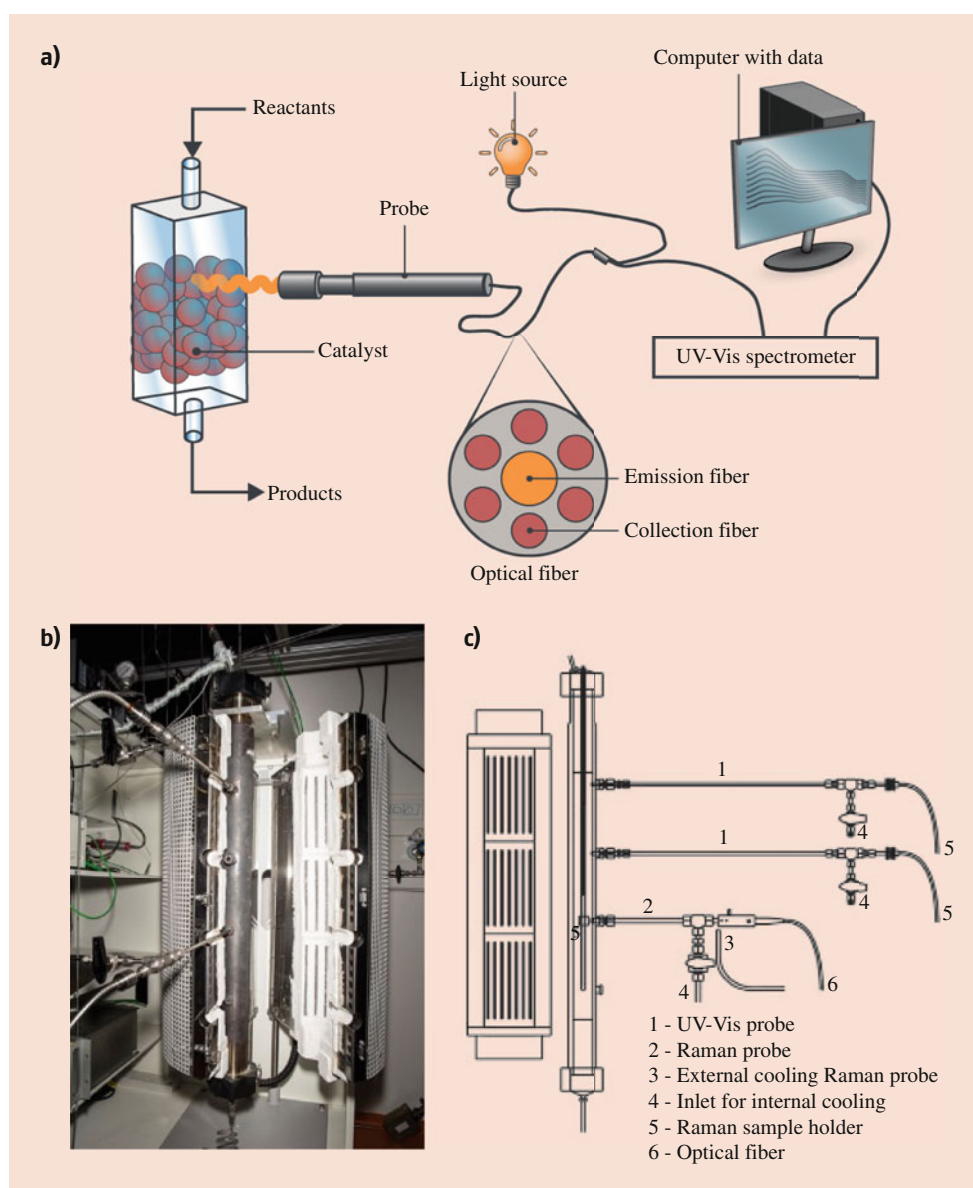
Micro-Spectroscopy

Optical microscopes can be upgraded to a UV-Vis microscope (i.e., a micro-spectrophotometer) by sending the incoming radiation from the microscope to a spectrometer, as shown in Fig. 11.5. In this way, a range of different spectroscopic techniques can be utilized with a much smaller sampling area (e.g., 1×1 μm) than possible with standard bench-top spectroscopy tools. This principle works with transmission, reflection, fluorescence, and other types of optical emission. As such, microscope spectrophotometers can be designed to measure UV-Vis-NIR spectra of microscopic samples or microscopic areas of larger objects, such as catalyst extrudates or pellets, as well as large crystals. A good example of the latter materials is the study of Mores et al. on single zeolite H-ZSM-5 crystals in the Methanol-to-Olefins (MTO) reaction [37]. Figure 11.5 shows an overview of the type of micro-spectroscopic information that can be obtained for this reaction studying individual zeolite H-ZSM-5 crystals as a function of both time and space. The gradual coloration of the zeolite crystals could be linked to the specific formation of hydrocarbon pool species and deactivating coke species, which are known to be relevant in the hydrocarbon pool mechanism of the MTO process. Specifically, the authors distinguished between graphite-like coke deposited on the external crystal surface and aromatic species, which are partially charged (i.e., carbocation species) formed inside the zeolite channels. Differences were noted between the central body and edges of the zeolite H-ZSM-5 crystals, as well as for different reaction temperatures, and even for different Si/Al ratios of the zeolite materials under study.

11.3 Probe Molecule UV-Vis Spectroscopy

Probe molecule spectroscopy has been widely used as a versatile technique to probe the structure of active sites in solid catalysts [38]. It is best known in combination with infrared (IR) spectroscopy, where molecules such as CO, NO, NH_3, and pyridine, are used to probe the surface chemistry of solid catalysts at different temperatures, and often in combination with a temperature programmed desorption (TPD) procedure. This methodology has allowed the in-depth investigation of the coordination environment of, e.g., supported transition metal ions, such as Cu^{2+}, and also to estimate the number of Brønsted and Lewis acid sites in

zeolite-based catalysts. Within this context it is somewhat surprising that the same approach has not been frequently used in combination with UV-Vis spectroscopy. Recently, Velthoen et al. reported pyridine UV-Vis spectroscopy as a novel methodology to study the acidic properties of solid acid catalysts [39a]. Pyridine was found to be an excellent probe molecule, as upon its interaction with acidic sites a significant shift in the electronic properties of pyridine could be observed with UV-Vis spectroscopy. It was found that pyridinium ions form on Brønsted acid sites, that pyridine coordinated to Lewis acid sites, and that pyridine hydrogen-bonded to surface hydroxyl groups. Physisorbed pyridine was also observed. In this way, a wide range of important,

Fig. 11.4 (**a**) Schematic of optical fiber UV-Vis spectroscopy of a solid catalyst placed in a plug-flow reactor; (**b**) Picture of a pilot-scale reactor, consisting of optical fiber technology to measure the changes in a catalytic bed taking place during reaction with operando UV-Vis and Raman spectroscopy as a function of bed height. The reactor is ~1 m long with four openings to insert probes (two of which are in use in this photograph, as presented by Sattler et al. [15, 16]; and (**c**) Schematic of the *operando* reactor setup, as illustrated in **b**). (Reproduced from [35, 36]; with permission from Wiley-VCH)
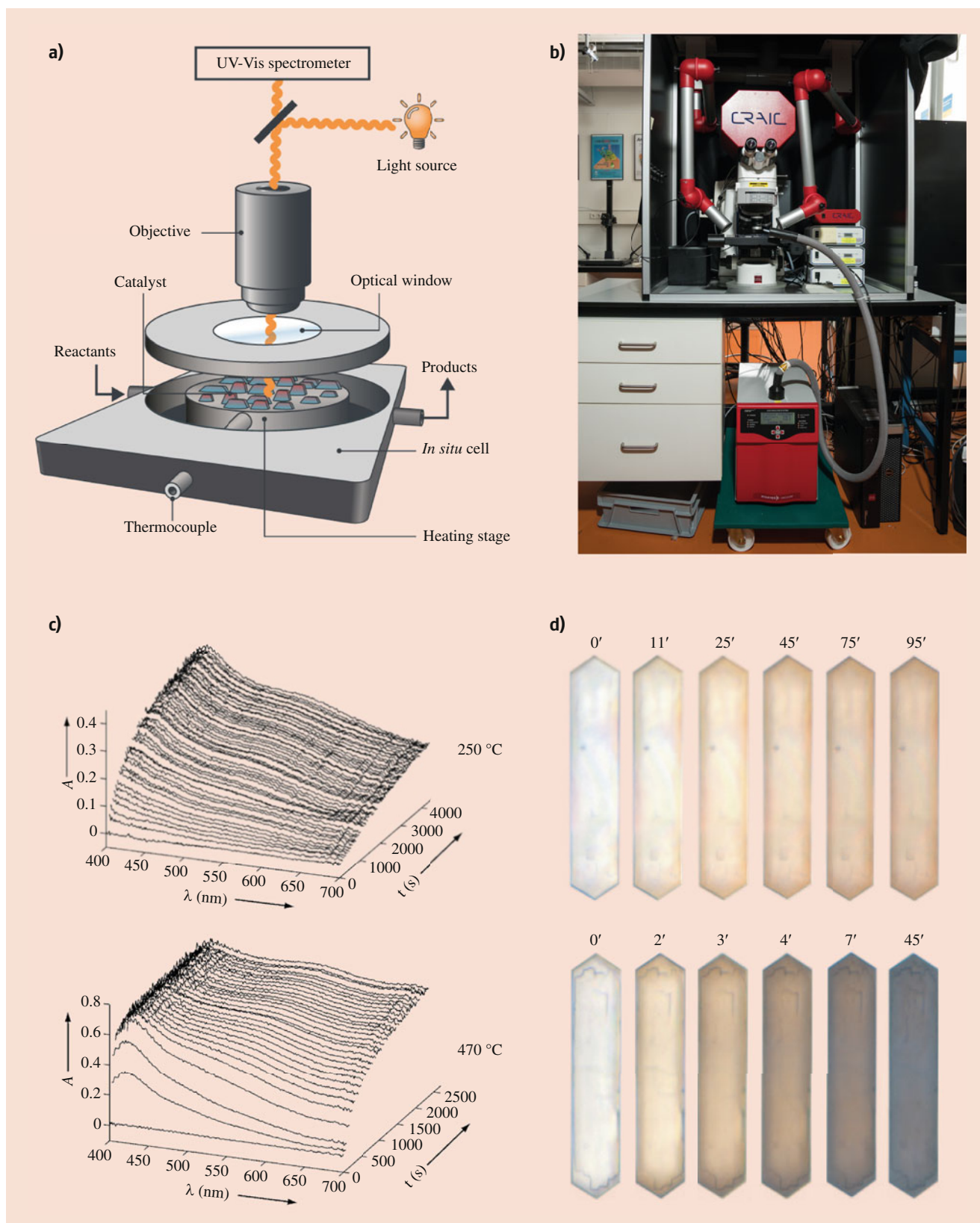
Fig. 11.5 (**a**) Schematic of a UV-Vis micro-spectroscopy setup, including an *In situ* or *operando* cell for measuring solid catalysts at work; (**b**) Picture of the *operando* UV-Vis micro-spectroscopy setup, including the reaction cell and online mass spectrometry (MS) analysis; (**c**) *Operando* UV-Vis spectra taken at two different reaction temperatures for the methanol-to-olefins (MTO) reactions over a single zeolite H-ZSM-5

catalytically relevant characteristics of solid acid catalysts could be probed, and even quantified. After removal of physisorbed pyridine and pyridine adsorbed to hydroxyl groups using a TPD treatment, quantification of the Lewis- and Brønsted-acidity was possible. Such a probe molecule is desirable because conventional acidity probing methods, such as NH_3-TPD and pyridine FT-IR spectroscopy, show only small differences in acidic properties for such solid acid catalysts. As such, the additional use of UV-Vis spectroscopy with respect to the application of pyridine FT-IR spectroscopy allows to distinguish not only between the Brønsted and Lewis acid sites as in the more classical pyridine FT-IR spectroscopy, but also between different weak acid sites. Other examples of probe molecules in combination with UV-Vis spectroscopy are CO for the determination of exposed gold sites on TiO_2 by studying changes in the surface plasmon resonance [39b], and the use of N-bromobenzyl substituted (E)-4′-hydroxy-4-stilbazolium bromide (NBSB) has also been reported to test the basicity of nitrogen organic compounds grafted on mesoporous cellular foam silica (MCF) [39c].

11.4 Coupling UV-Vis Spectroscopy with Other Analytical Methods

UV-Vis spectroscopy requires relatively low photon fluxes and energies, and therefore the chances of interfering with the catalyst system under study are much lower than for, e.g., X-ray absorption spectroscopy. The coupling of relevant *in situ* or *operando* spectroscopies (e.g., X-ray absorption, FT-IR and UV-Vis spectroscopy for their relative ease of use and broad applicability) with computational methods like density functional theory (DFT) has yielded important insights in many types of catalytic systems [10]. Several review papers summarize the coupling of *operando* and *in situ* UV-Vis spectroscopy with other analytical methods [40], and we refer to these articles for a more comprehensive overview of the field.

An example is the much-debated active site in/for the conversion of methane to methanol, which typically takes place in Cu-exchanged zeolites. *In situ* UV-Vis and resonance Raman (rR) spectroscopy, in combination with DFT calculations, have granted a unique insight into the complex, enzyme-like structure of the active site in Cu-based zeolites by Schoonheydt, Solomon, Sels, and co-workers [41, 42a]. This work, recently summarized in a review paper [43], is illustrated in Fig. 11.6 for zeolite ZSM-5

and mordenite loaded with Cu-ions. *In situ* UV-Vis spectroscopy has been instrumental in the discovery of the hydroxylation of methane into methanol over Cu-based zeolites, as illustrated in Fig. 11.6a for Cu-ZSM-5. It was found that in an O_2 or N_2O environment an intense absorption feature at ~22,700 cm^{-1} was formed, which decays in the presence of methane. By using deuterated and non-deuterated methane, it was possible to demonstrate a H/D kinetic isotope effect that is consistent with C-H cleavage in the rate-limiting step. The 22,700 cm^{-1} absorption band was subsequently interpreted in different ways, but the definitive assignment to a $[Cu_2O]^{2+}$ cluster was only possible when the UV-Vis spectroscopy was combined with DFT calculations as well as rR spectroscopy (Fig. 11.6b). Furthermore, this cluster motif is not only present in Cu-ZSM-5, but also in other zeolites, such as Cu-mordenite. However, here the situation is more complex as there are two spectroscopic features in the 22,000 cm^{-1} range, namely, one at ~21,900 cm^{-1} and one at ~23,100 cm^{-1} each having a different decay rate as a function of temperature (Fig. 11.6c, d). By again combining these *in situ* UV-Vis spectroscopy data with rR spectroscopy experiments, it was possible to identify the nature of the two $[Cu_2O]^{2+}$ clusters in mordenite, which are very similar to those found in zeolite ZSM-5. Based on all the results obtained, a reaction mechanism for methane hydroxylation could be proposed, as summarized in Fig. 11.6e. The role and state of copper species in zeolites for the oxidation of methane to methanol is still being actively researched [42b, c].

The coupling of UV-Vis spectroscopy with other characterization methods has become particularly facile, as discussed above, with the use of optical fiber technology. This is illustrated in Fig. 11.7 for the combination of *operando* Raman and UV-Vis spectroscopy to investigate Cr/Al_2O_3 catalysts during the dehydrogenation of propane into propene at elevated temperatures [29]. With these two methods, two processes could be evaluated simultaneously; on the one hand, the formation of coke deposits could be measured, while the typical d-d transitions of reduced Cr-species present in the active catalyst could be monitored. The unique aspect of this setup is that the decrease in diffuse reflectance can be directly used to quantify the measured Raman spectra, thereby allowing for a semiquantitative analysis of the Raman data [29, 44]. This approach/ principle can also be extended to other methods, such as X-ray absorption spectroscopy (XAS) [45].

Fig. 11.5 (continued) crystal, indicating the formation of different hydrocarbon pool species, and related deactivation products; and (**d**) Optical images of the zeolite crystals at the two different reaction temperatures as a function of time when exposed to methanol. (Reproduced from [37]; with permission from Wiley-VCH)
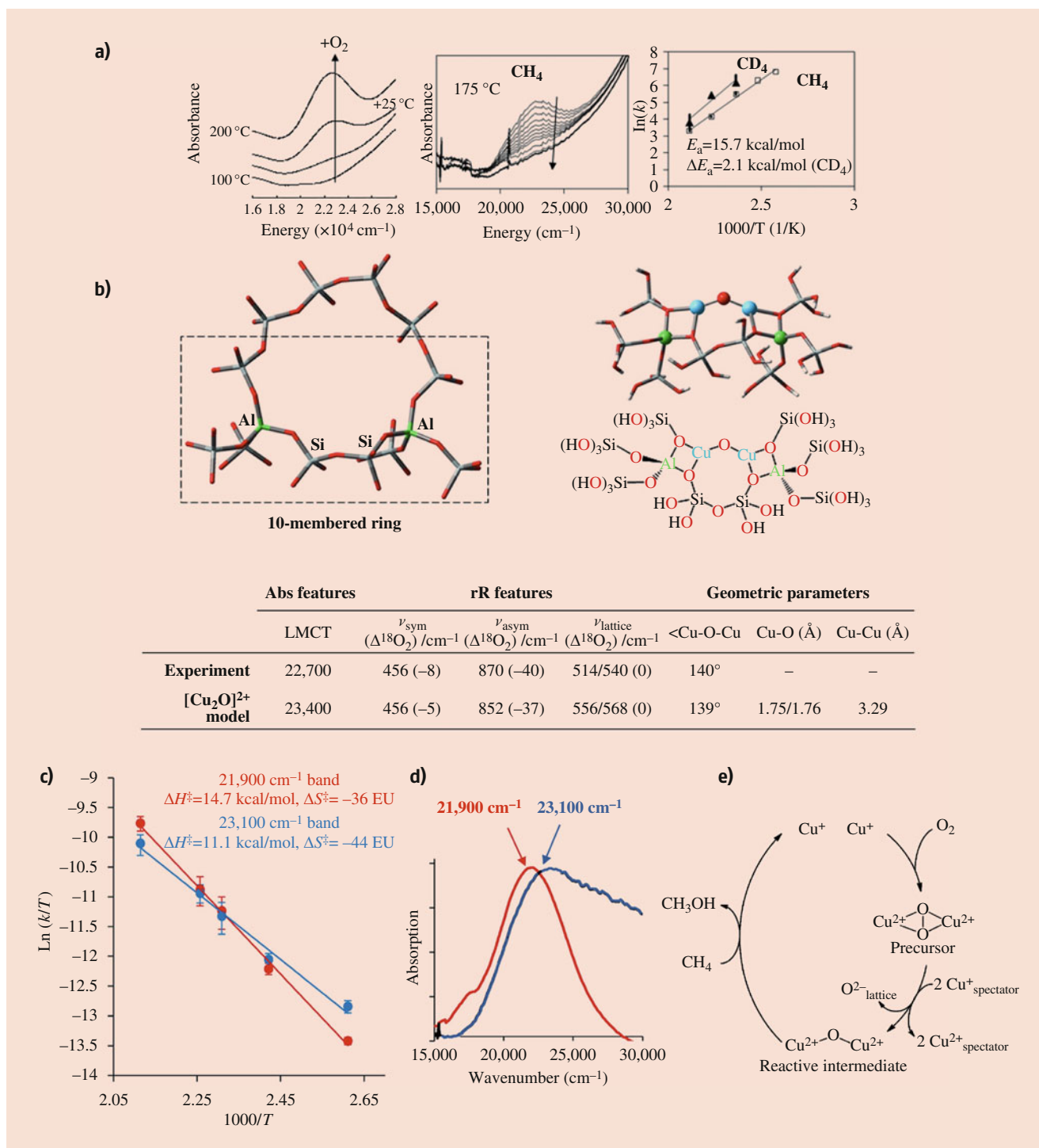
Abs features		rR features			Geometric parameters		
	LMCT	ν_{sym} $(\Delta^{18}O_2)$ /cm^{-1}	ν_{asym} $(\Delta^{18}O_2)$ /cm^{-1}	$\nu_{lattice}$ $(\Delta^{18}O_2)$ /cm^{-1}	<Cu-O-Cu	Cu-O (Å)	Cu-Cu (Å)
Experiment	22,700	456 (−8)	870 (−40)	514/540 (0)	140°	–	–
[Cu₂O]²⁺ model	23,400	456 (−5)	852 (−37)	556/568 (0)	139°	1.75/1.76	3.29

Fig. 11.6 *Operando* UV-Vis spectroscopy for monitoring the changes taking place in a Cu-ZSM-5 zeolite material during the oxidation of methane into methanol. (**a**) The 22,700 cm^{-1} absorption band is formed in the presence of O$_2$ and disappears in the presence of CH$_4$, and differences are noted between CH$_4$ and CD$_4$ illustrating a H/D kinetic isotope effect; (**b**) Schematic representation of the ten-membered ring motif in the zeolite ZSM-5 lattice, in which the methane activation reaction takes place, including the [Cu₂O]²⁺ cluster model derived from this motif, based on combined UV-Vis and resonance Raman (rR) spectroscopy, including theoretical calculations; (**c**) Correlation of two different UV-Vis spectral features (i.e., a 21,900 and 23,100 cm^{-1} absorption band) and their relation to the activation energy by an Arrhenius plot for the Cu-mordenite zeolite system active in methane activation; (**d**) The two different absorption bands present in the Cu-mordenite zeolite system. The red spectrum is measured during heating in an oxygen environment at elevated temperatures, while the blue spectrum is measured when switching from an oxygen to a helium environment at elevated temperatures; and (**e**) The proposed reaction mechanism for oxygen activation and methane hydroxylation forming methanol, based on the performed spectroscopic measurements, including *operando* UV-Vis spectroscopy, and theoretical work. (Reproduced from [41]; with permission from American Chemical Society)

Fig. 11.7 (**a**) A schematic overview of a combined *operando* UV-Vis/Raman spectroscopy setup for measuring a solid catalyst reacting with gases at elevated temperatures; (**b**) Side photograph of such a quartz reactor, filled with catalyst material, with optical windows used in this *operando* setup; and (**c**) Time-resolved DR-UV-Vis spectra recorded from the *operando* UV-Vis/Raman setup as shown in (**a**) and (**b**), which represent the deactivation of the solid material. The catalyst material shown in (**b**) and (**c**) is a Cr/Al_2O_3 propane dehydrogenation catalyst, which possess characteristic d-d transitions of reduced Cr-species, which are present under typical propane dehydrogenation catalysis conditions
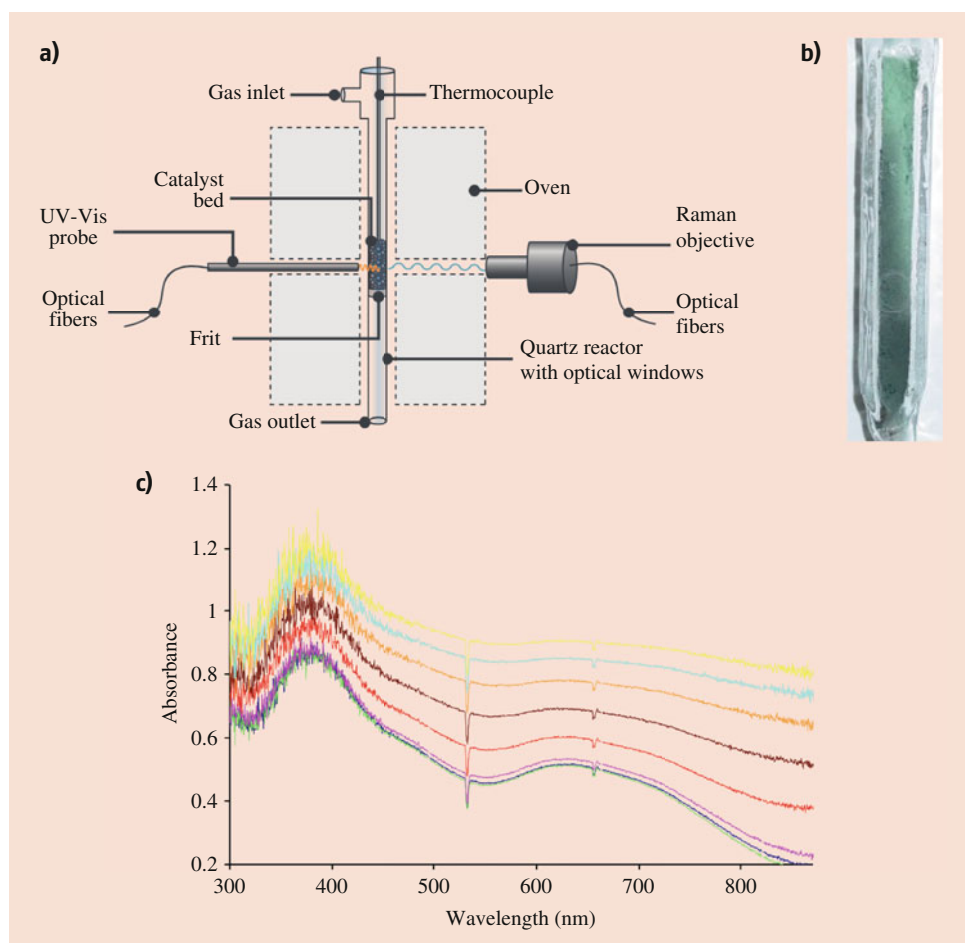
Another good example of such combined spectroscopy approach is the coupling/simultaneous operation of UV-Vis spectroscopy with both attenuated Total Reflection Fourier-transform Infrared (ATR-FT-IR) spectroscopy and ESR by the group of Brückner, where the gas-liquid phase transformation of benzyl alcohol was studied over a copper/TEMPO catalyst (TEMPO = (2,2,6,6-tetra-methylpiperidin-1-yl)oxyl) [46a]. Within this context, it is important to mention the latest example from the Brückner group. In this work, in cooperation with the beamline scientists at the Soleil Synchrotron (France), the authors show the successful coupling of *operando* UV-Vis spectroscopy with *operando* ATR-IR, EPR, and XAS to gain in depth information on the copper/TEMPO catalyst system [46b]. This is also a clear technical achievement as an EPR spectrometer had to be placed in the Rock Beamline of Soleil.

While aims and hypotheses vary greatly in their nature throughout catalysis research, some basic rules of thumb for designing a combined spectroscopic study on an industrial catalyst material may be considered. For example, the combination of *in situ* spectroscopies into one setup is preferred, yet only if the addition of several spectroscopies does not significantly alter in any way the catalysis taking place in the reactor,

nor decrease the signal-to-noise ratio of either spectroscopic technique. Quantification of the catalytic process (activity, selectivity) to ensure working conditions relevant to industrial spectroscopy should be prioritized as only then the analytical data obtained can be correlated with confidence with catalytic performance. Finally, it is possible with combined setups to evaluate the effect of one analytical technique on the catalyst with another one by evaluating the separate contributions of the analytical techniques. It is important to realize that measuring is always to some extent also perturbing the system.

Another recent example of the coupling of multiple spectroscopic techniques (i.e., Raman spectroscopy, UV-Vis spectroscopy, XAS, DRIFTS, and temperature programmed surface reaction (TPSR) spectroscopy) demonstrated that the events that occurred in a solid catalyst during the polymerization of olefins [7, 47]. Here the group of Wachs used DFT to propose a new initiation mechanism for ethylene polymerization, which was corroborated by the spectroscopic results. A similar combination of techniques proved useful for the identification of surface anchoring sites on ReO_x catalysts for propylene metathesis, namely Raman spectroscopy, DRIFTS, and near-ambient-pressure-X-ray photoelectron spectroscopy (NAP-XPS) were combined [7]. Zhang

and Wachs found that ReO_4 sites were most likely the most active site for propylene metathesis by studying a range of different supports, and chemically probing reactants under dehydrated conditions and olefin metathesis reaction conditions via *in situ* UV-Vis spectroscopy [7, 48].

Another example involves the coupling of UV-Vis spectroscopy with X-ray diffraction (XRD), as shown in a recent study which correlated the formation of hydrocarbon pool species with the lattice expansion in small-pore zeolite cages during the MTO reaction [49]. More specifically, the formation of the retained hydrocarbon pool species during the MTO process at a reaction temperature of 400 °C was followed using *operando* UV-Vis spectroscopy. During the same experiment, using *operando* XRD, the expansion of the zeolite framework was assessed, and the activity of the catalyst was measured using online GC. In this way, it was possible to determine which species were responsible for the lattice expansion for all the different small-pore zeolite samples under study, and thus which species (i.e., different methylated naphthalenes and pyrenes) were likely blocking the large zeolite cages leading to zeolite deactivation [18]. Furthermore, by combining *operando* UV-Vis spectroscopy with FT-IR spectroscopy, Qian et al. were able to unravel the role of methoxy and aromatic species in the MTO reaction over zeotype H-SAPO-34 materials. It was found that there is an induction period yielding mainly methanol, methoxy, and protonated dimethyl ether species, whereas poly-alkylated benzenes and poly-aromatic species are found in the active phase of the MTO reaction over H-SAPO-34. In this manner, the distinct reaction pathways responsible for the formation of olefins and poly-aromatics could be established, these species are present during the entire MTO process, and coupling both spectroscopic techniques (UV-Vis and IR spectroscopy) revealed that both catalytic routes are directly related to the amount of surface poly-alkylated benzene carbocations and methoxy species.

different species (potentially) present in convoluted *in situ* or *operando* spectra.

An example of a combined experiment-theory study was recently given/published by Velthoen et al., who studied a multitude of different metallocene structures, which are sandwich complexes of a group 4 transition metal (e.g., Zr) and cyclopentadienyl-derived ligands [50]. Some of these molecular structures are shown in Fig. 11.8. Via the application of DFT and UV-Vis diffuse reflectance spectroscopy, the authors were able to build a library of several different complexes. By subsequently simulating UV-Vis spectra, their greatly convoluted experimentally obtained spectra could finally be understood. They were hereby able to link the formation $AlMe_2^+$ to the activity of the polymer catalysts. The active catalytic complex undergoes several activation steps in a complex scheme. Cl ligand abstraction by $AlMe_2^+$ eventually forms active, and dormant species, which once more react with $AlMe_2^+$ in a delicate balance between the active species and the polymeric form. Finally, they also showed that the degree of activation of these catalysts is not always 100%, or uniform.

Another illustrative example showing the importance of corroboration between theory and experiment is a study on single-crystal ZSM-5 zeolites with styrene oligomerization as probe reaction, where it was found that the activity and selectivity of the Brønsted acid-catalyzed oligomerization of styrene-derived molecules is controlled by the steric properties of intra-zeolite micropore voids as well as by the side groups on the aromatic rings (e.g., methoxy group vs. fluorine group) [51, 52]. DFT computations, futher corroborated by synchrotron-based IR micro-spectroscopy data, showed that the preference for a particular reaction mechanism in the oligomerization of styrene is determined by the local shape of zeolite micropores, which explained the experimentally observed orientation-dependent UV-Vis absorption intensities throughout a single zeolite H-ZSM-5 crystal, as shown in Fig. 11.9. It was found that the dimeric carbocation is preferentially formed within the straight channels of zeolite H-ZSM-5.

11.5 Complementing Data Interpretation with Density Functional Theory

As one of the downsides of *in situ* and *operando* UV-Vis spectroscopy in catalysis is the overlap of many important spectral features, leaving the spectra convoluted and difficult to discern, it is imperative to have excellent references as well as relevant model compounds. Such references and model compounds sometimes prove to be very difficult to obtain experimentally, as, e.g., the reaction intermediate species (temporally) stabilized by the catalysts might be the desired reference species, but unfortunately no such pure compound can be simply bought nor synthesized. As such, DFT has proven to be an important tool to discriminate between the

11.6 Application of Chemometrics and Multivariate Analyses

As is the case with the application of nearly every spectroscopic technique to study catalysis, the ultimate goal is to establish certain structure–activity relationships in order to design new and improved catalysts. Yet to fully appreciate the potential information that can be extracted from such techniques, particularly when applying UV-Vis spectroscopy under catalytic reaction conditions, systematic experiment design coupled with mathematical and statistical routines is likely necessary. Advances are being made in the application of chemometrics, which is the chemical discipline that uses mathematical and statistical methods to employ formal logic
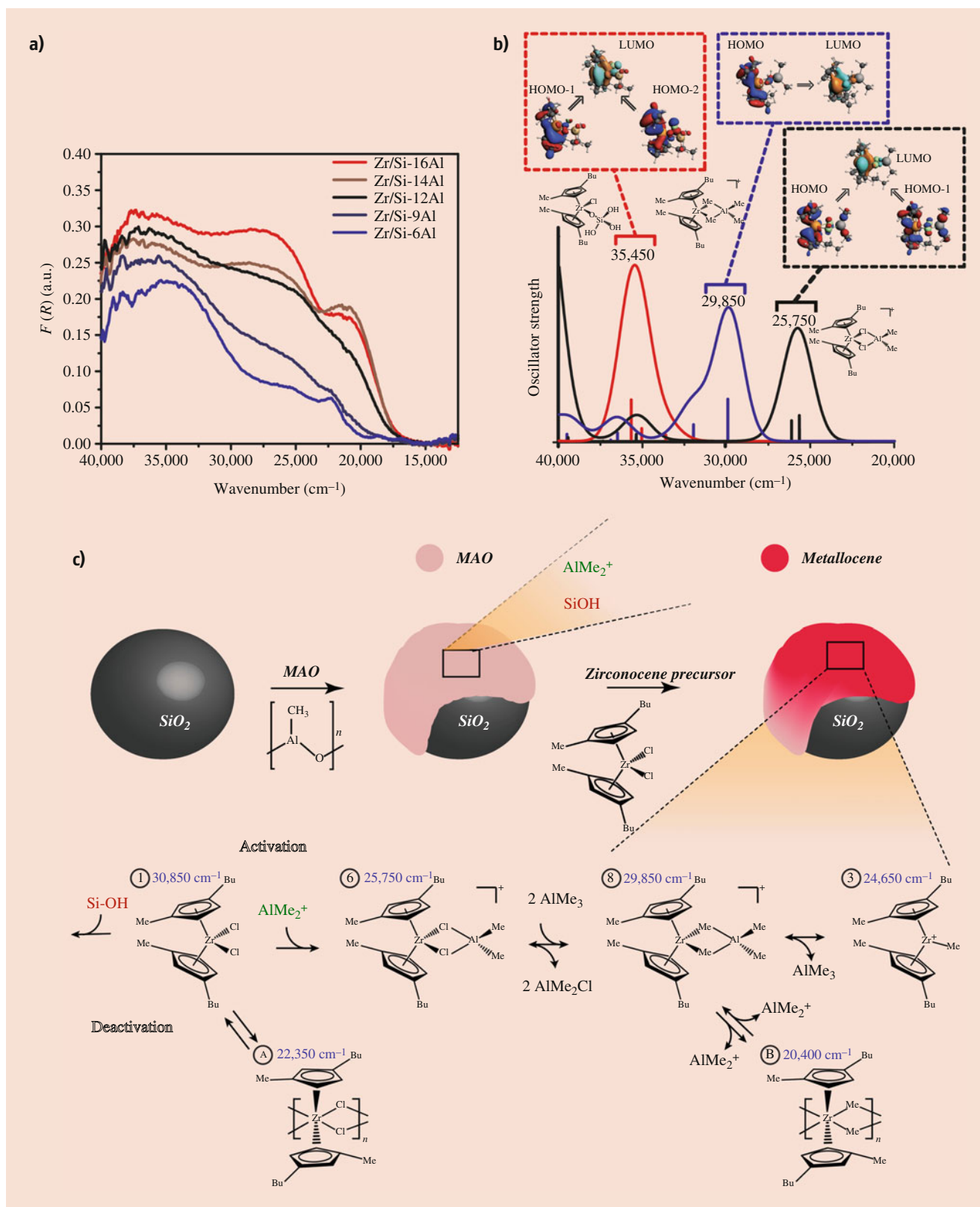
Fig. 11.8 UV-Vis diffuse reflectance spectroscopy was used to study the activation of metallocene-based polymerization catalysts by co-catalyst methylaluminoxane (MAO): (**a**) UV-Vis diffuse reflectance spectra for different loadings of co-catalyst; (**b**) The vertical excitation energies that were calculated with time-dependent density functional theory (DFT) for the different possible MAO-activated metallocene complexes; and (**c**) Schematic overview of the stepwise activation of metallocene catalysts by the MAO co-catalyst by combining *In situ* UV-Vis diffuse reflectance spectroscopy and DFT calculations. (Reproduced from [50]; with permission from Elsevier)
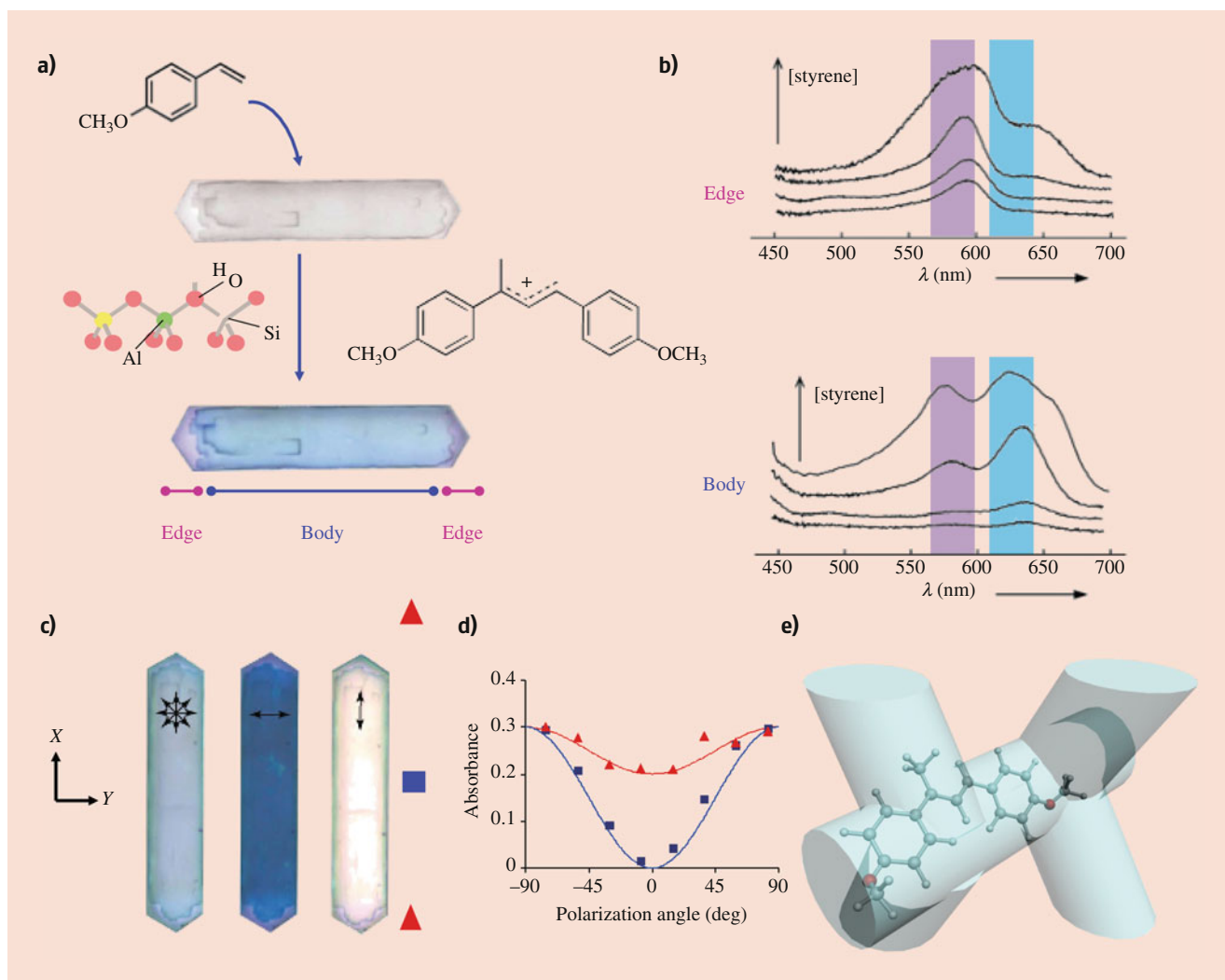
Fig. 11.9 Shape selectivity and catalytic activity trends as revealed within the pores of single zeolite H-ZSM-5 crystals by time- and space-resolved UV-Vis micro-spectroscopy. (**a**) Styrene oligomerization was taken as a selective probe reaction, of which the oligomerized product, formed on the Brønsted acid sites within the zeolite pores, is UV-Vis absorbing; (**b**) Spatial differences were found to occur in the main body of the H-ZSM-5 crystals with respect to the crystal edges, which was confirmed by density functional theory (DFT) calculations to stem from differences in zeolite acidity in different pore orientations; (**c**) Visible differences in orientation-dependent activity were also found; (**d**) Polarization angle in degrees, and the absorbance of the UV-Vis bands at 580 nm and 630 nm, as demonstrated in (**c**), thereby showing the preferential orientation of the dimeric styrene carbocation in the straight pores of zeolite ZSM-5; and (**e**) Schematic representation of the pores of a single zeolite ZSM-5 crystal shows an explanation for the observed orientation effects and the position of the dimeric species in the straight pore. (Reproduced from [52]; with permission from Wiley-VCH)

to, disentangle (deconvolute) relevant chemical information (in our case convoluted UV-Vis spectra).

A good example demonstrating such an approach is the study of the activation and deactivation mechanisms of Methanol-to-Olefins (MTO) catalyzed by several different small-pore zeolites by Goetze et al. [53] Three different zeolite catalysts were studied (i.e., CHA, DDR, and LEV frameworks), which all have relatively large cages, interconnected by small, 8-ring windows. These three MTO catalysts were studied at reaction conditions between 350 °C and 450 °C, coupling the time-resolved measurement of UV-Vis spectra with online GC. By analyzing the time-resolved UV-Vis spectra with Multivariate Curve Resolution (MCR), and deconvoluting the data matrix of the complete time series of the *operando* UV-Vis spectra into contributions of pure components, as shown in Fig. 11.10, this analysis procedure provided a decomposition that maximizes the explained variance in the data with the option to define constraints to such a decomposition. By defining these constraints as physically or chemically meaningful (e.g., non-negativity and unimodality of spectral features) the set of spectra could be split into two experimentally meaningful parts: first, components comprising UV-Vis spectral features that follow the same kinetics during the reaction, and second,
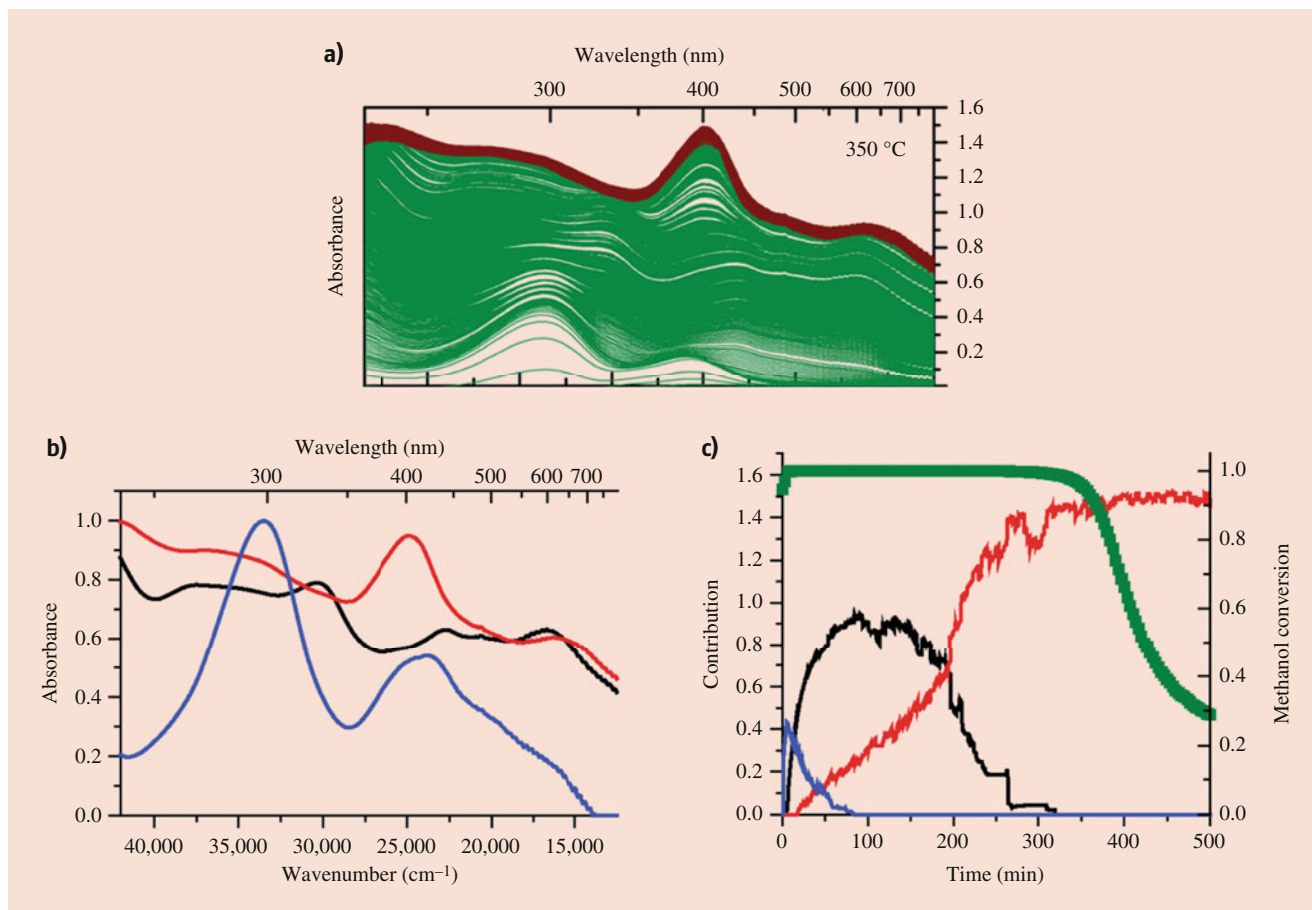
Fig. 11.10 (**a**) UV-Vis spectra (as measured by fiber-optics) of a methanol-to-olefins (MTO) reaction at 350 °C over a CHA-zeolite; (**b**) the multivariate curve resolution components; and (**c**) their respective (time-resolved) contributions are shown on the right. (Reproduced from [53]; with permission from American Chemical Society)

the contribution of these components versus time. In this way, a large dataset containing hundreds or even thousands of spectra can be demodulated into chemically meaningful spectral groups. By performing this analysis procedure, the authors were able to group together specific spectral features that have relevance to different periods of time in the MTO reaction, e.g., the induction period where a hydrocarbon pool is formed, and the reaction period where this pool of hydrocarbon species produces olefins/produces the desired olefins.

11.7 Selected Applications of UV-Vis Spectroscopy in the Field of Catalysis

UV-Vis spectroscopy is a widely applicable characterization technique with relevance not only to heterogeneous catalysis, but also very much to homogeneous catalysis, electrocatalysis, and even photocatalysis. In what follows, we will highlight some recent research work for each of these fields of catalysis.

11.7.1 Heterogeneous Catalysis

Several examples of the application of UV-Vis spectroscopy in heterogeneous catalysis have already been given throughout this chapter. In this subsection, we will focus on some recent applications of UV-Vis spectroscopy in novel manners, or studying novel type of catalyst materials. For example, heterogeneous catalysts in industrial applications often come in the form of macroscopic pellets or catalyst extrudates, which are shaped bodies of the solid catalyst material. The active phase is often combined with a binder material, such as a clay mineral (e.g., kaolinite) and an amorphous oxide (e.g., silica and alumina). These catalyst extrudates are on the scale of millimeters or centimeters. It is known that the performance of zeolite-based catalyst extrudates can be greatly influenced by the choice of binder material, but *operando* spectroscopy studies are relatively scarce, despite the enormous industrial impact of binder effects. Verkleij et al. studied binder effects in zeolite ZSM-5-bound catalyst extrudates by using *operando* UV-Vis micro-spectroscopy measurements, using the setup

described in Fig. 11.5 [54–56]. Verkleij and co-workers presented a new methodology to investigate such complex effects, by studying the oligomerization of ethylene as well as the transalkylation of aromatics in catalyst extrudates at different reaction pressures using *operando* UV-Vis microspectroscopy coupled with online GC analysis. SiO_2-bound extrudates were shown to form polyaromatic coke species throughout the catalyst extrudates homogeneously, while for the Al_2O_3-bound catalyst extrudates a ring of coke formed, which moved inward with reaction time. The results are summarized in Fig. 11.11.

As catalysis is a multiscale phenomenon, from the Ångstrom scale where chemical bonds are broken and formed, to the nanometers of supported nanoparticular catalysts, to centimeters of catalyst extrudates, to meters of chemical reactors, it is important to obtain more insights in spatial heterogeneities across a reactor bed, as discussed above for Cr/Al_2O_3 catalyst extrudates for propane dehydrogenation reactions [35, 36]. As such, it is interesting not only to probe intra-catalyst extrudate differences, such as done by Verkleij et al. [54–56], but also to probe differences on a larger scale such as at different points in a chemical reactor. Goetze and Weckhuysen studied the formation of polyaromatic coke species under reaction conditions at three different points in a catalytic reactor, while monitoring the reaction products by online GC. In this study, two types of zeolite-based catalyst materials, H-ZSM-5 and Mg-ZSM-5, were compared [57]. For both of the reactions, it was shown that a coke-front forms at the beginning of the reactor, and then travels through the catalyst bed. As soon as the coke front reached the end of the reactor, catalyst deactivation was found to occur. The Mg-modified ZSM-5 catalyst showed a longer catalyst lifetime and higher selectivity toward olefins, which was accompanied by slower coke-front formation throughout the catalyst bed.

In a study combining solid-state NMR spectroscopy and *operando* UV-Vis diffuse-reflectance spectroscopy, electrophilic aromatic substitution was studied in the zeolite-catalyzed bioethanol-mediated benzene ethylation process [58a]. Chowdhury et al used UV-Vis diffuse reflectance spectroscopy to identify and differentiate between neutral and carbocationic organic species that were trapped within the zeolite material, and the gas-phase products that were formed during the ethylation of benzene with ethanol over zeolite H-ZSM-5 extrudates at 300 °C for 30 min. During this experiment, absorption bands at 295, 334, 415, and 596 nm were observed, which which became more intense with increasing time-on-stream. After approximately 7 min of reaction, the only observed increase was the absorption band at 596 nm. The three other absorption bands at 295, 334, and 415 nm were attributed to neutral or charged alkylated benzenes, while the band at 596 nm could later on be confirmed to develop due to π-complexes between the zeolites and aromatic species (and further confirmed by ^{13}C

magic angle spinning solid state nuclear magnetic resonance). Using this combined spectroscopy approach together with differently substituted aromatic compounds, a controversial Wheland-type intermediate was confirmed to exist within the zeolite framework (i.e., a cyclohexadienyl cation that appears as a reactive intermediate in electrophilic aromatic substitution). More details on the identification of this Wheland-type reaction intermediate can be found in Fig. 11.12. A theoretical interpretation for these experimental findings on the Wheland-type intermediate have been recently given by Van Speybroeck and co-workers [58b].

Another interesting combined *in situ* study was provided by the group of Jentoft, who have investigated the formation and reactivity of unsaturated carbenium ions in zeolite H-ZSM-5 [59a, b]. This was made possible by the use of *in situ* UV-Vis and FT-IR spectroscopy, which by careful inspection of the data allowed for the identification of three types of unsaturated carbenium ions, namely, acylic monoenyl cations, acylic dienyl cations, and cyclopentenyl cations. Interestingly, highly suitable reference spectra of these unsaturated carbenium ions could be generated in sulfuric acid, and hence could serve as fingerprints for their identification in zeolite H-ZSM-5. Moreover, several linear correlations could be inferred from the UV-Vis spectroscopy data between the number of the carbons in a particular carbocation and the position of the π ➜ π* transition. These insights were used to monitor the formation and reactivity of alkyl-substituted cyclopentenyl cations from a dimethyloctatriene precursor. Two types of cations were observed, in which the C-2 of the allylic system was either proton- or methyl-substituted.

When electrons at the interface between negative and positive permittivity materials are stimulated by incident radiation, a surface plasmon resonance can be excited/activated. This surface plasmon is an electromagnetic surface wave that propagates out of the surface, and as it propagates out of this interface between material and the external medium (gas, liquid, vacuum), it can be very sensitive to any change of this boundary such as the adsorption of molecules to the surface. Gold is a material that is known to exhibit surface plasmon resonance, which can be excited by UV-Vis radiation. Au plasmon peaks have recently been used to study the adsorption of hydrogen and oxygen on small gold nanoparticles supported on different supports [59c]. By combining *in situ* UV-Vis spectroscopy with a geometric model of the Au nanoparticles, evidence was found for adsorption of H_2 and O_2 at the gold-support perimeters. Gold clusters exhibiting a localized surface plasmon resonance band at around 520 nm in the presence of $NaBH_4$ were found to do so by electron doping to the Au sp band, which was caused by adsorbed H atoms to the gold nanoclusters [59d]. Plasmon resonance has proved to be a particularly useful phenomenon for surface-enhanced spectroscopies, like surface-enhanced Raman spectroscopy.
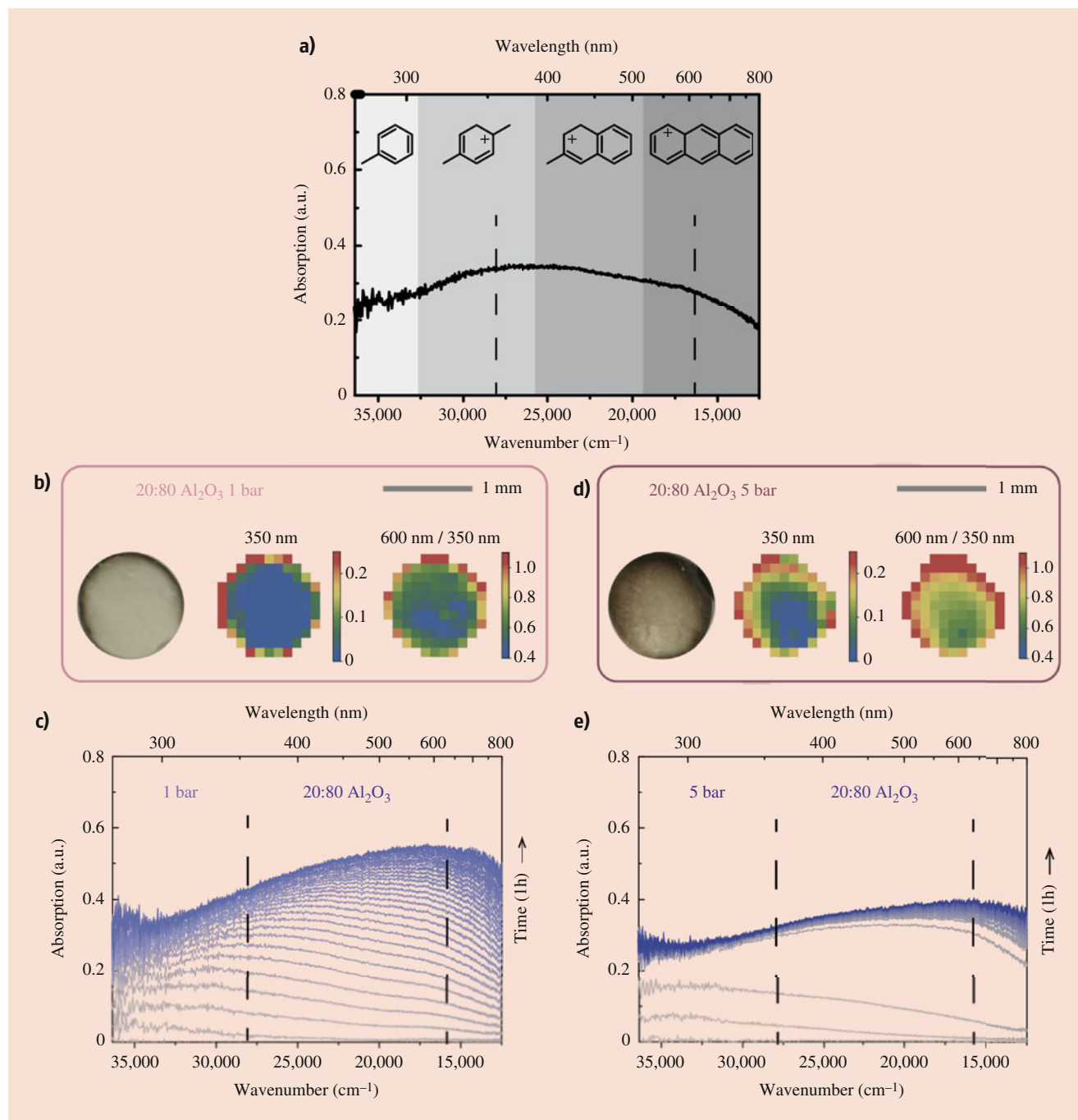
Fig. 11.11 High-pressure *operando* UV-Vis micro-spectroscopy study of coke formation in extrudates during the transalkylation of aromatics: (**a**) Schematic of the different molecules that contribute to the DR-UV-Vis spectroscopy during the reaction of toluene and 1,2,4-trimethylbenzene. Panels (**b**) and (**d**) show the cross sections of alumina-bound catalyst extrudates at 1 and 5 bar, respectively, while Panels (**c**) and (**e**) show their respective *operando* UV-Vis spectra. (Reproduced from [55, 56]; with permission from Wiley-VCH)

11.7.2 Homogeneous Catalysis

In homogeneous catalysis, experiments can (in principle) be performed in a cuvette. Yet as for heterogeneous catalysis, the ease of use of fiber optics, and the possibility they bring to combine several spectroscopic characterization techniques (like, e.g., ATR-IR, and Raman spectroscopy) in one experiment, is becoming more and more popular for homogeneous catalysis experiments [60]. Some examples include the work on homogeneous Cu-, Cr- and Mo-catalysts by the group of Tromp et al. [61] Other illustrative examples of homogeneous catalytic reactions characterized by UV-Vis spectroscopy probes are performed by the
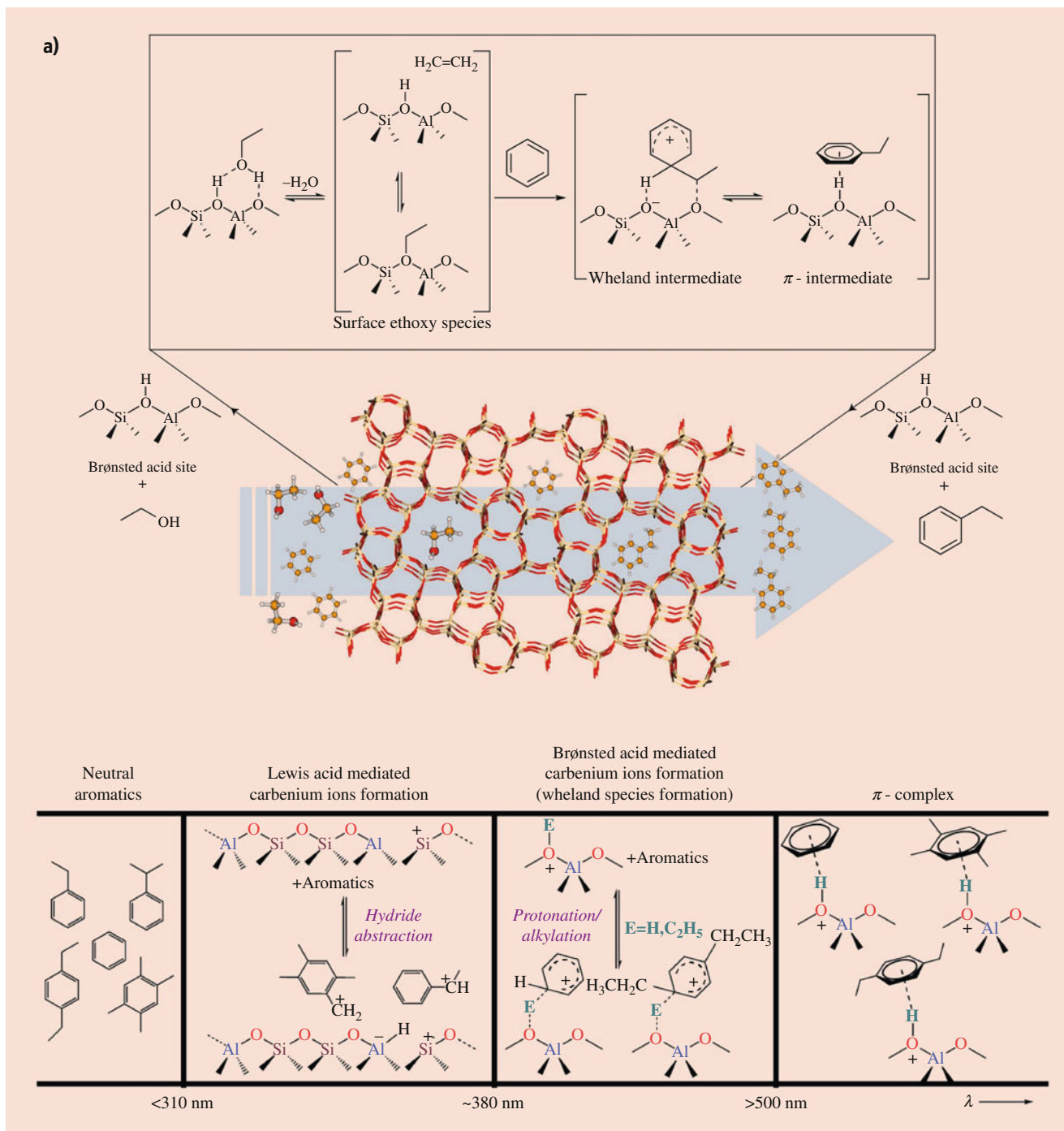
Fig. 11.12 (**a**) Proposed reaction mechanism, based on *operando* UV-Vis spectroscopy and NMR, including an overview of the possible intermediates identified to be of importance during the ethylation of benzene with ethanol, including the controversial Wheland-type intermediate; (**b**) *Operando* UV-Vis spectroscopy measurements during the ethylation of benzene with ethanol at 300 °C during the first 10 min, and the following 20 min; and (**c**) Electronic effect on the formation of a Wheland-type intermediate as corroborated by *operando* UV-Vis spectroscopy when benzene, ethylbenzene, and methoxybenzene are compared. (Reproduced from [58]; with permission from Nature)

group of Brückner, who investigated the gas-liquid phase transformation of benzyl alcohol by a copper/TEMPO catalyst (TEMPO = (2,2,6,6-tetramethylpiperidin-1-yl)oxyl) [46].

Rabeah et al. set out to understand the role of TEMPO using a sequential approach, studying different components of the active catalytic mixture separately. They found that the sharp metal-to-
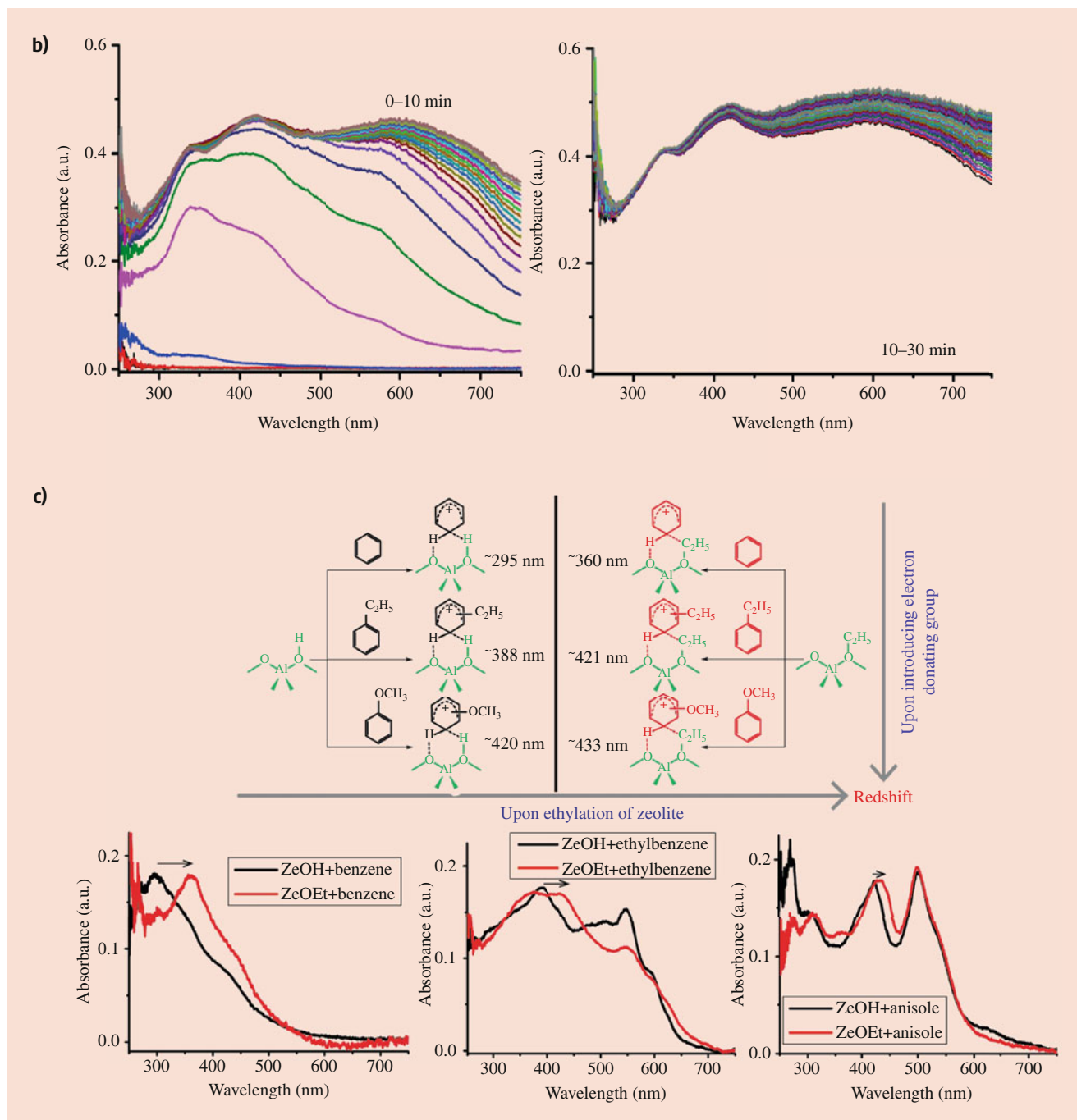
Fig. 11.12 (continued)

ligand charge-transfer (MLCT) band at 310 nm was an excellent indicator of the formation of a Cu⁺ site bpy defined, which did not seem to interact with TEMPO. By performing such experiments also with *in situ* EPR, the team was able to corroborate a new reaction mechanism for alcohol oxidation over the complex $Cu^+OTf/bpy/NMI/TEMPO/O_2$ catalytic system.

The impact of Al activators on the structure of $Cr(acac)_3$ catalyst precursor for ethylene oligomerization was also assessed with fiber optics UV-Vis spectroscopy [62]. In these experiments the d-d transition of Cr^{3+}, as well as intra-ligand transitions and LMCT bands, could be probed. Limitations of the setup (most likely overabsorption in the range of interest) did not allow for probing by *in situ* UV-Vis spectroscopy of the reaction, but rather the formation of catalyst precursors before starting the reaction could be followed; however the limitation of UV-Vis spectroscopy in

this case was that the coordination of Cr is not accessible by this technique and as such the results were combined with *in situ* ATR-IR and XAS.

11.7.3 Electrocatalysis

In electrocatalysis, electron transfers are the driving force. As such, UV-Vis spectroscopy is highly relevant for electrocatalysis, and has been applied more and more with the increasing importance of electrocatalysis. Setups for electrocatalysis may be similar to all those described above for homogeneous catalysis, or heterogeneous catalysis, with fiber optic probes, or diffuse-reflectance accessories, granted that the electrode must allow the collection of UV-Vis radiation. Transparent films like ITO should be easier to measure even in transmission than, e.g., black glassy carbon. A recent example is that of Ni-Mo catalysts employed as noble-metal alternative for water-splitting reactions [63]. The downside of this catalyst is its rapid deactivation, and as such *in situ* characterization of the catalysts was performed in combination with atomic force microscopy (AFM) [28], and several other relevant characterization techniques [38]. Via the application of *in situ* UV-Vis spectroscopy authors found that multiple processes were onset by a higher negative potential, a lower degree of Mo oxidation, as well as an increase in local pH at the cathode due to higher hydrogen evolution reaction (HER) activity at higher negative potentials. Both of these processes cause Mo leaching, which was confirmed with *in situ* UV-Vis spectroscopy [28]. *In situ* UV-Vis spectroscopy measurements were also performed on the related oxygen evolution reaction (OER) by another group, where the electronic structure of two Co-containing catalysts could be probed under working conditions [64]. The $Zn_{0.35}Co_{0.65}O$ and $CoAl_2O_4$ catalyst materials were measured at different oxidizing potentials and spectra were compared to *ex situ* measurements to identify important transformations during reaction. For example, the Wurtzite-type $Zn_{0.35}Co_{0.65}O$ material undergoes a structural transformation upon the introduction to the 1 M KOH electrolyte material, from pure tetrahedral Co^{2+} coordination, to an octahedral Co^{2+} coordination without changing its oxidation state.

11.7.4 Photocatalysis

In photocatalysis, the acceleration of a photochemical reaction is achieved in the presence of a catalyst; either catalyzed photolysis where incoming radiation is absorbed by an adsorbed molecule, or in photogenerated catalysis, which relies on the creation of an electron hole-pair to generate free radicals, which are then able to undergo secondary reactions. The splitting of water by a.o. TiO_2 makes photocatalysis

practically applicable, although the search for materials to make such processes economically viable and therefore practically applied is still ongoing. Nevertheless, in photocatalysis applications, the analysis of semiconductors, and properties like band gaps are extremely interesting and often of direct relevance to the catalytic properties. These, as we know from what is described in the subsections above, are features that can be examined by UV-Vis spectroscopy.

Recently, a new analytical approach was published, which combines the *in situ* measurement of NMR spectroscopy, UV-Vis spectroscopy, and illumination of the sample, which allows simultaneous and time-resolved detection of paramagnetic and diamagnetic species relevant to photocatalysis, as shown in Fig. 11.13 [65]. Seegerer et al. demonstrated the properties and relevance of this setup to photocatalysis by studying the photocatalytic reduction of 4-bromo-benzaldehyde through a N,N-bis(2,6-diisopropylphenyl)-perylene-3,4,9,10-bisdicarboximide (PDI) catalyst and could obtain *in situ* kinetic information of both paramagnetic (PDI) and diamagnetic (reactant and product) constituents relevant to the catalytic reaction. Their solution included a 5 mm ambered NMR tube that was flanked by radiofrequency coils. Inside this 5 mm NMR tube, a reflection dip probe UV-Vis illumination and detection probe was fitted. In this way, by illuminating and subsequently measuring *in situ* UV-Vis spectra, UV-Vis spectra were obtained with a time resolution of ~15 s. Another example is the *in situ* study of the photodegradation of Aldrich humic acids, which was used as a model compound for natural organic matter. By studying the reaction *in situ*, the authors were able to determine that the photodegradation of these compounds occurred, and also the presence of likely byproducts forming from the degradation [66].

11.8 Conclusions and Outlook

UV-Vis spectroscopy is an extremely versatile, relatively easy to use spectroscopic technique of which the spectrometers enjoy economic acquisition prices... Hence, they are more and more used in academic and industrial labs to investigate catalysts in various shapes and forms and also for various applications. Over the past two decades, significant advances have been made in the application of *in situ* and *operando* UV-Vis spectroscopy to unravel the organic and inorganic part of catalysts at work. In this chapter, we have shown that the coupling of UV-Vis spectroscopy with a range of other important spectroscopies is possible and very relevant to several kinds of catalysis, and particularly the opportunities with fiber-optic UV-Vis spectroscopy are almost endless. The onset of data analysis techniques, such as multivariate curve resolution, a form of multivariate analysis, opens doors for complex, convoluted, time-resolved experiments that are of great importance for catalysis.

Fig. 11.13 (**a**) Schematic of a combined *In situ* NMR/UV-Vis spectroscopy for performing photocatalytic experiments; (**b**) Overview of the NMR tube that contains all spectroscopic and illumination components; and (**c**) Related UV-Vis spectra obtained by this combined NMR/UV-Vis setup. (Reproduced from [65]; with permission from Wiley-VCH)
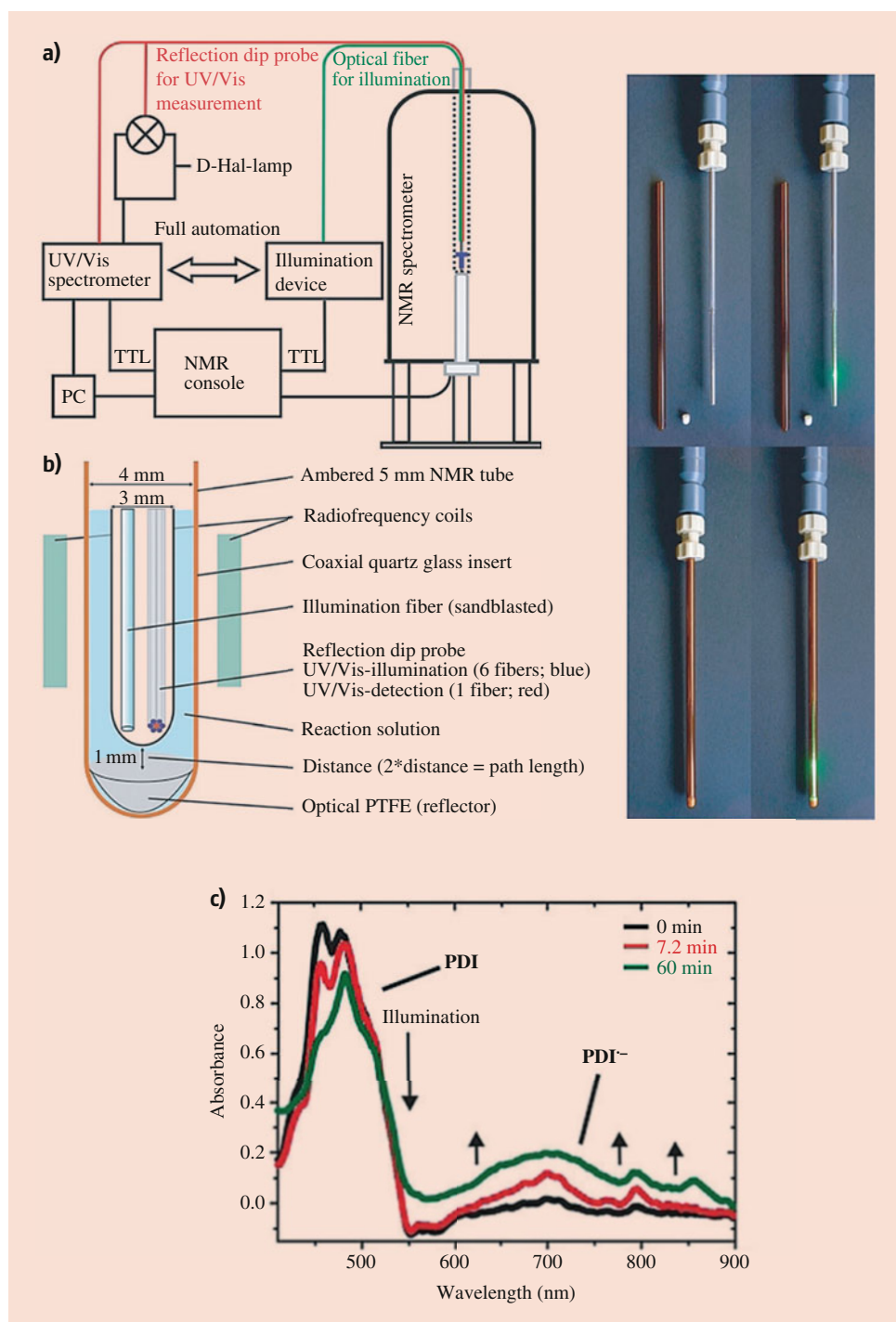
Furthermore, there is extensive theory available to describe and predict UV-Vis spectra, making the application of precise data analysis possible to an increasingly greater extent. One can anticipate that neural networks and artificial intelligence, combined with on-line UV-Vis spectroscopy measurements may lead to reduced times for new catalyst discovery and the understanding of both reaction and deactivation phenomena for industrially important processes. Time-resolution can be pushed below the sub-second regime with still acceptable spectral resolution and intensities, while the potential coupling with Atomic Force Microscopy (AFM), as is currently possible with IR, Raman, and fluorescence spectroscopy, will make it possible to perform nanoscale UV-Vis spectroscopy to unravel spatial heterogeneities within solid catalysts.

The development of *in situ* or *operando* techniques exists primarily to close the temperature, pressure, and materials

11

gaps that exist in our fundamental knowledge of chemical reactions and their dynamics. The developments in UV-Vis spectroscopy over the past two decades, particularly due to the application of fiber-optics, have shown to bridge that gap for some important chemical reactions, allowing scientists to study reactions under truly realistic industrial conditions (e.g., high temperature and pressure) and even on industrially relevant samples (e.g., catalyst extrudates). Transient UV-Vis experimentation in which pulses of reactive gases are rapidly interchanged with inert gases will also enable researchers to distinguish between active species and related reaction intermediates and spectator species, which are not involved in the reaction mechanism. Finally, with the rising importance of electrocatalysis as well as photocatalysis for our energy and materials needs, the possibility to probe electronic excitations with UV-Vis spectroscopy may prove to play an important role in the synthesis as well as the characterization improvement loop in the search for such improved catalysts in the coming decades. Hence, the future of UV-Vis spectroscopy and microscopy in the broad field of catalysis is bright and certainly will help to realize the energy and materials transition needed to make our society more circular and sustainable [67].

References

1. (a) Gauglitz, G., Vo-Dinh, T. (eds.): Handbook of Spectroscopy. Wiley-VCH, Weinheim (2003); (b) Atkins, P., de Paula, J., Keeler, J.: Physical Chemistry, 11th edn. Oxford University Press, Oxford (2014)
2. Hollas, J.M.: Modern Spectroscopy, 4th edn. Wiley, Chichester (2004)
3. (a) Verberckmoes, A.A., Weckhuysen, B.M., Schoonheydt, R.A.: Spectroscopy and coordination chemistry of cobalt in molecular sieves. Microporous Mesoporous Mater. **22**, 165–178 (1998); (b) Schoonheydt, R.A.: Transition-metal ions in zeolites: siting and energetics of Cu^{2+}. Catal. Rev. Sci. Eng. **35**, 129–168 (1993)
4. (a) Bonneviot, L., Legendre, O., Kermarec, M., Olivier, D., Che, M.: Characterization by UV-Vis-NIR reflectance spectroscopy of the exchange sites of nickel on silica. J. Colloid Interface Sci. **134**, 534–547 (1990); (b) Boujday, S., Lambert, J.F., Che, M.: Amorphous silica as a versatile ligand for Ni-II amine complexes: toward interfacial molecular recognition. ChemPhysChem. **5**, 1003–1013 (2004)
5. (a) Groppo, E., Lamberti, C., Bordiga, S., Spoto, G., Zecchina, A.: The structure of active centers and the ethylene polymerization mechanism on the Cr/SiO_2 catalyst: a frontier for the characterization methods. Chem. Rev. **105**, 115–183 (2005); (b) Groppo, E., Zecchina, A., Barzan, C., Vitillo, J.G.: Low temperature activation and reactivity of CO_2 over a Cr^{II}-based heterogeneous catalyst: a spectroscopic study. Phys. Chem. Chem. Phys. **14**, 6538–6543 (2012)
6. (a) Dedecek, J., Sobalik, Z., Wichterlova, B.: Siting and distribution of framework aluminium atoms in silicon-rich zeolites and impact on catalysis. Catal. Rev. Sci. Eng. **54**, 135–223 (2012); (b) Dedecek, J., Kaucky, D., Wichterlova, B.: Co^{2+} ion siting in pentasil-containing zeolites, part 3. Co^{2+} ion sites and their occupation in ZSM-5: a Vis diffuse reflectance spectroscopy study. Microporous Mesoporous Mater. **35**, 483–494 (2000)
7. (a) Ross-Medgaarden, E.I., Wachs, I.E.: Structural determination of bulk and surface tungsten oxides with UV-vis diffuse reflectance spectroscopy and Raman spectroscopy. J. Phys. Chem. C. **111**, 15089–15099 (2007); (b) Wachs, I.E.: Dalton Trans. **42**, 11762–11769 (2013); (c) Lee, E.L., Wachs, I.E.: *In situ* spectroscopic investigation of the molecular and electronic structures of SiO_2 supported surface metal oxides. J. Phys. Chem. C. **111**, 14410–14425 (2007)
8. (a) Khodakov, A., Yang, J., Su, S., Iglesia, E., Bell, A.T.: Structure and properties of vanadium oxide zirconia catalysts for propane oxidative dehydrogenation. J. Catal. **177**, 343–351 (1998); (b) Khodakov, A., Olfhof, B., Bell, A.T., Iglesia, E.: J. Catal. **181**, 205–216 (1999)
9. Sojka, Z., Bozon-Verduraz, F., Che, M.: UV-Vis-NIR and EPR spectroscopies. In: Ertl, G., Knözinger, Schüth, F., Weitkamp, J. (eds.) *Handbook of Heterogeneous Catalysis*, vol. 2, pp. 1039–1065. Wiley-VCH, Weinheim (2008)
10. Burns, R.G.: Mineralogical Applications of Crystal Field Theory, 2nd edn. Cambridge University Press, Cambridge (1993)
11. Klokishner, S.L., Reu, O., Chan-Thaw, C.E., Jentoft, F.C., Schlögl, R.: Redox properties of manganese-containing zirconia solid solution catalysts analyzed by *in situ* UV-Vis spectroscopy and crystal field theory. J. Phys. Chem. A. **115**, 8100–8112 (2011)
12. Jentoft, F.C.: In: Che, M., Védrine, J.C. (eds.) *Characterization of Solid Materials and Heterogeneous Catalysts: From Structure to Surface Reactivity*, 1st edn, pp. 89–147. Wiley-VCH, Weinheim (2012)
13. Schoonheydt, R.A.: UV-Vis-NIR spectroscopy and microscopy of heterogeneous catalysts. Chem. Soc. Rev. **39**, 5051–5066 (2010)
14. Jentoft, F.C.: Ultraviolet-visible-near infrared spectroscopy in catalysis: theory, experiment, analysis and application under reaction conditions. Adv. Catal. **52**, 129–211 (2009)
15. Schoonheydt, R.A.: Diffuse reflectance spectroscopy. In: Delannay, F. (ed.) *Characterization of Heterogeneous Catalysts*, pp. 125–160. Marcel Dekker, New York (1984)
16. Kellermann, R.: Diffuse reflectance and photoacoustic spectroscopies. In: Delgass, W.N., Haller, G.L., Kellermann, R., Lunsford, J.H. (eds.) *Spectroscopy in Heterogeneous Catalysis*, pp. 86–131. Academic Press, New York (1979)
17. Klier, K.: Reflectance spectroscopy as a tool for investigating dispersed solids and their surfaces. Catal. Rev. Sci. Eng. **1**, 207–232 (1968)
18. Kortüm, G.: Reflectance Spectroscopy. Springer, Berlin (1969)
19. Weckhuysen, B.M., Schoonheydt, R.A.: Recent progress in diffuse reflectance spectroscopy of supported metal oxide catalysts. Catal. Today. **49**, 441–451 (1999)
20. Weckhuysen, B.M., Schoonheydt, R.A.: Electronic spectroscopies. In: Weckhuysen, B.M., Van der Voort, P., Catana, G. (eds.) *Spectroscopy of Transition Metal Ions on Surfaces*, pp. 221–268. Leuven University Press, Leuven (2000)
21. Weckhuysen, B.M.: Ultraviolet-visible spectroscopy. In: Weckhuysen, B.M. (ed.) In Situ Spectroscopy of Catalysts, pp. 255–270. American Scientific Publishers, Stevenson Ranch (2004)

22. (a) Banares, M.A.: Operando methodology: Combination of *in situ* spectroscopy and simultaneous activity measurements under catalytic reaction conditions. Catal. Today. **10**, 71–77 (2005); (b) Weckhuysen, B.M.: Determining the active site in a catalytic process: *Operando* spectroscopy is more than a buzzword. *Phys. Chem. Chem. Phys.* **5**, 4351–4360 (2003)

23. Förster, H., Seebode, J., Fejes, P., Kiricsi, I.: Formation of carbocations from C3 compounds in zeolites of different acidities. J. Chem. Soc. Faraday Trans. **83**, 1109–1117 (1987)

24. Melsheimer, J., Ziegler, D.: Ethene transformation on HZSM-5 studied by combined UV-Vis spectroscopy and on-line gas chromatography. J. Chem. Soc. Faraday Trans. **88**, 2101–2108 (1992)

25. Sendoda, Y., Ono, Y., Keii, T.: Properties of nickel cations in X-zeolite as studied by electronic spectroscopy. J. Catal. **39**, 357–362 (1975)

26. Weckhuysen, B.M., Bensalem, A., Schoonheydt, R.A.: *In situ* UV-Vis diffuse reflectance spectroscopy-online activity measurements: significance of Cr^{n+}-species (n = 2, 3 and 6) in n-butane dehydrogenation catalyzed by supported chromium oxide catalysts. J. Chem. Soc. Faraday Trans. **94**, 2011–2014 (1998)

27. Weckhuysen, B.M., Verberckmoes, A.A., Debaere, J., Ooms, K., Langhans, I., Schoonheydt, R.A.: *In situ* UV-Vis diffuse reflectance spectroscopy-on line activity measurements of supported chromium oxide catalysts: relating isobutane dehydrogenation activity with Cr-speciation via experimental design. J. Mol. Catal. A: Chemical. **151**, 115–131 (2000)

28. Bruckner, A.: Simultaneous combination of *in-situ* EPR/UV-Vis/on line GC: a novel setup for investigating transition metal oxide catalysts under working conditions. Chem. Commun., (20), 2122–2123 (2001)

29. Nijhuis, T.A., Tinnemans, S.J., Visser, T., Weckhuysen, B.M.: *Operando* spectroscopic investigation of supported metal oxide catalysts by combined time-resolved UV-Vis/Raman/online mass spectrometry. Phys. Chem. Chem. Phys. **5**, 4361–4365 (2003)

30. Bruckner, A.: Monitoring transition metal ions (TMI) in oxide catalysts during (re)action: the power of *operando* EPR. Phys. Chem. Chem. Phys. **5**, 4461–4472 (2003)

31. Melsheimer, J., Thiede, M., Ahmad, R., Tzolova-Müller, G., Jentoft, F.C.: Improved experimental setup for *in situ* UV-Vis-NIR spectroscopy under catalytic conditions. Phys. Chem. Chem. Phys. **5**, 4366–4370 (2003)

32. Vogt, C., Weckhuysen, B.M., Ruiz-Martinez, J.: Effect of feedstock and catalyst impurities on the methanol-to-olefin reaction over H-SAPO-34. ChemCatChem. **9**, 183–194 (2017)

33. Weckhuysen, B.M., Baetens, D., Schoonheydt, R.A.: Spectroscopy of the formation of microporous transition metal ion containing aluminophosphates under hydrothermal conditions. Angew. Chem. Int. Ed. **39**, 3419–3422 (2000)

34. Puurunen, R.L., Beheydt, B.G., Weckhuysen, B.M.: Monitoring chromia/alumina catalysts *in-situ* during propane dehydrogenation by optical fiber UV-visible diffuse reflectance spectroscopy. J. Catal. **204**, 253–257 (2001)

35. Sattler, J.J.H.B., et al.: *Operando* UV-Vis spectroscopy of a catalytic solid in a pilot-scale reactor: deactivation of a CrO_x/Al_2O_3 propane dehydrogenation catalyst. Chem. Commun. **49**, 1518–1520 (2013)

36. Sattler, J.J.H.B., Mens, A.M., Weckhuysen, B.M.: Real-time quantitative operando Raman spectroscopy of a CrO_x/Al_2O_3 propane dehydrogenation catalyst in a pilot-scale reactor. ChemCatChem. **6**, 3139–3145 (2014)

37. (a) Mores, D., Stavitski, E., Kox, M.H.F., Kornatowski, J., Olsbye, U., Weckhuysen, B.M.: Space- and time-resolved *in-situ* spectroscopy on the coke formation in molecular sieves: methanol-to-olefin conversion over H-ZSM-5 and H-SAPO-34. Chem. Eur. J. **14**, 11320–11327 (2008); (b) Mores, D., Kornatowski, J., Olsbye, U., Weckhuysen, B.M.: Coke formation during het methanol-to-olefin conversion: *in situ* micro-spectroscopy on individual H-ZSM-5

crystals with different Brønsted acidity. Chem. Eur. J. **17**, 2874–2884 (2011)

38. (a) Niemantsverdriet, J.W.: *Spectroscopy in Catalysis, An Introduction*, 3rd edn. Wiley-VCH, Weinheim (2007); (b) Che, M., Védrine, J.C. (eds.): *Characterization of Solid Materials and Heterogeneous Catalysts: From Structure to Surface Reactivity*, 1st edn. Wiley-VCH, Weinheim (2012)

39. (a) Velthoen, M.E.Z., Nab, S., Weckhuysen, B.M.: Probing acid sites in solid catalysts with pyridine UV-Vis spectroscopy. Phys. Chem. Chem. Phys. **20**, 21647–21659 (2018); (b) Lari, G.M., Nowicka, E., Morgan, D.J., Kondrat, S.A., Hutchings, G.J.: The use of carbon monoxide as a probe molecule in spectroscopic studies fro determination of exposed gold sites on TiO_2. *Phys. Chem. Chem. Phys.* **17**, 23236–23244 (2015); (c) Stawicka, K., Prukala, D., Siodla, T., Sikorski, M., Ziolek, M.: UV-Vis spectroscopy combined with azastilbene probe as a tool for testing basicity of mesoporous silica modified with nitrogen compounds. Appl. Catal. A General. **570**, 339–347 (2019)

40. (a) Bentrup, U.: Combining *in situ* characterization methods in one setup: looking with more eyes into the intricate chemistry of the synthesis and working of heterogeneous catalysts. Chem. Soc. Rev. **39**, 4718–4730 (2010); (b) Tinnemans, S.J., Mesu, J.G., Kervinen, K., Visser, T., Nijhuis, T.A., Beale, A.M., Keller, D.E., van der Eerden, A.M.J., Weckhuysen, B.M.: Combining *operando* techniques in one spectroscopic-reaction cell: new opportunities for elucidating the active site and related reaction mechanism in catalysis. Catal. Today. **113**, 3–15 (2006)

41. Groothaert, M.H., Smeets, P.J., Sels, B.F., Jacobs, P.A., Schoonheydt, R.A.: Selective oxidation of methane by the bis(μ-oxo)dicopper core stabilized on ZSM-5 and mordenite zeolites. J. Am. Chem. Soc. **127**, 1394–1395 (2005)

42. (a) Woertink, J.S., et al.: A $[Cu_2O]^{2+}$ core in Cu-ZSM-5, the active site in the oxidation of methane to methanol. Proc. Natl. Acad. Sci. **106**, 18908–18913 (2009); (b) Brezicki, G., Kammert, J.D., Gunnoe, B., Paolucci, C., Davis, R.J.: Insights into the speciation of Cu in the Cu-H-mordenite catalyst for the oxidation of methanol to methanol. *ACS Catal.* **9**, 5308–5319 (2019); (c) Grundner, S., Markovits, M.A.C., Li, G., Tromp, M., Pidko, E.A., Hensen, E.J.M., Jentys, A., Sanchez-Sanchez, M., Lercher, J.A.: Single-site trinuclear copper oxygen clusters in mordenite for selective conversion of methane to methanol. *Nat. Commun.* **6**, 7546 (2015)

43. Snyder, B.E.R., Bols, M.L., Schoonheydt, R.A., Sels, B.F., Solomon, E.I.: Iron and copper active sites in zeolites and their correlation to metalloenzymes. Chem. Rev. **118**, 2718–2768 (2018)

44. (a) Nijhuis, T.A., Tinnemans, S.J., Visser, T., Weckhuysen, B.M.: Towards real-time spectroscopic process control for the dehydrogenation of propane over supported chromium oxide catalysts. Chem. Eng. Sci. **59**, 5487–5492 (2004); (b) Tinnemans, S.J., Kox, M.H.F., Nijhuis, T.A., Visser, T., Weckhuysen, B.M.: Real time quantitative Raman spectroscopy of supported metal oxide catalysts without the need for an internal standard. Phys. Chem. Chem. Phys. **7**, 211–216 (2005)

45. Beale, A.M., van Der Eerden, A.M.J., Kervinen, K., Newton, M.A., Weckhuysen, B.M.: Adding a third dimension to *operando* spectroscopy: a combined UV-Vis, Raman and XAFS setup to study heterogeneous catalysts under working conditions. Chem. Commun., (24), 3015–3017 (2005)

46. (a) Rabeah, J., Bentrup, U., Stößer, R., Brückner, A.: Selective alcohol oxidation by a copper TEMPO catalyst: mechanistic insights by simultaneously coupled *operando* EPR/UV-Vis/ATR-IR spectroscopy. Angew. Chem. Int. Ed. **54**, 11791–11794 (2015); (b) Rabeah, J., Briois, V., Adomeit, S., La Fontaine, C., Bentrup, U., Brückner, A.: Multivariate analysis of coupled *operando* EPR/XANES/EXAFS/UV-Vis/ATR-IR spectroscopy: a new dimension for mechanistic studies of catalytic gas-liquid phase reactions. Chem. Eur. J. **26**, 7395–7404 (2020)

47. Chakrabarti, A., Gierada, M., Handzlik, J., Wachs, I.E.: *Operando* molecular spectroscopy during ethylene polymerization by supported CrO$_x$/SiO$_2$ catalysts: active sites, reaction intermediates, and structure-activity relationship. Top. Catal. **59**, 725–739 (2016)

48. (a) Zhang, B., Wachs, I.E.: Identifying the catalytic active site for propylene metathesis by supported ReO$_x$ catalysts. ACS Catal. **11**, 1962–1976 (2021); (b) Zhang, B., Lwin, S., Xiang, S., Frenkel, A.I., Wachs, I.E.: Tuning the number of active sites and turnover frequencies by surface modification of supported ReO$_4$/(SiO$_2$-Al$_2$O$_3$) catalysts for olefin metathesis. ACS Catal. **11**, 2412–2421 (2021); (c) Lwin, S., Li, Y., Frenkel, A.I., Wachs, I.E.: Activation of surface ReO$_x$ sites on Al$_2$O$_3$ catalysts for olefin metathesis. ACS Catal. **5**, 6807–6814 (2015)

49. Goetze, J., Yarulina, I., Gascon, J., Kapteijn, F., Weckhuysen, B.M.: Revealing lattice expansion of small-pore zeolite catalysts during the methanol-to-olefins process using combined *operando* X-ray diffraction and UV-vis spectroscopy. ACS Catal. **8**, 2060–2070 (2018)

50. Velthoen, M.E.Z., Boereboom, J.M., Bulo, R.E., Weckhuysen, B.M.: Insights into the activation of silica-supported metallocene olefin polymerization catalysts by methylaluminoxane. Catal. Today. **334**, 223–230 (2019)

51. Buurmans, I.L.C., Pidko, E., de Groot, J.M., Stavitksi, E., van Santen, R.A., Weckhuysen, B.M.: Styrene oligomerization as a molecular probe reaction for zeolite acidity: a UV-Vis spectroscopy and DFT study. Phys. Chem. Chem. Phys. **12**, 7032–7040 (2010)

52. (a) Stavitski, E., Kox, M.H.F., Weckhuysen, B.M.: Revealing shape selectivity and catalytic activity trends within the pores of H-ZSM-5 crystals by time- and space-resolved optical and fluorescence microspectroscopy. Chem. Eur. J. **13**, 7057–7065 (2007); (b) Stavitksi, E., Pidko, E.A., Kox, M.H.F., Hensen, E.J.M., van Santen, R.A., Weckhuysen, B.M.: Detection of carbocationic species in zeolites: large crystals pave the way. Chem. Eur. J. **16**, 9340–9348 (2010)

53. Goetze, J., Meirer, F., Yarulina, I., Gascon, J., Kapteijn, F., Ruiz-Martinez, J., Weckhuysen, B.M.: Insights into the activity and deactivation of the methanol-to-olefins process over different small-pore zeolites as studied with *operando* UV-vis spectroscopy. ACS Catal. **7**, 4033–4046 (2017)

54. Verkleij, S.P., Whiting, G.T., Esclapez, S.P., Mertens, M.M., Bons, A.J., Burgers, M., Weckhuysen, B.M.: *Operando* microspectroscopy on ZSM-5 containing extrudates during the oligomerization of 1-hexene. Catal. Sci. Technol. **8**, 2175–2185 (2018)

55. Verkleij, S.P., Whiting, G.T., Pieper, D., Parres, E.S., Li, S.W., Mertens, M.M., Janssen, M., Bons, A.J., Burgers, M., Weckhuysen, B.M.: Chemical imaging of the binder-dependent coke formation in zeolite-based catalyst bodies during the transalkylation of aromatics. ChemCatChem. **11**, 4788–4796 (2019)

56. Verkleij, S.P., Whiting, G.T., Parres, E.S., Li, S.W., Mertens, M.M., Janssen, M., Bons, A.J., Burgers, M., Weckhuysen, B.M.: High-pressure operando UV-vis micro-spectroscopy of coke formation in zeolite-based catalyst extrudates during the transalkylation of aromatics. ChemCatChem. **12**, 5465–5475 (2020)

57. Goetze, J., Weckhuysen, B.M.: Spatiotemporal coke formation over zeolite ZSM-5 during the methanol-to-olefins process as studied with *operando* UV-Vis spectroscopy: a comparison between H-ZSM-5 and Mg-ZSM-5. Catal. Sci. Technol. **8**, 1632–1644 (2018)

58. (a) Chowdhury, A.D., Houben, K., Whiting, G.T., Chung, S.H., Baldus, M., Weckhuysen, B.M.: Electrophilic aromatic substitution over zeolites generates Wheland-type reaction intermediates. Nat. Catal. **1**, 23–31 (2018); (b) Bocus, M., Vanduyfhuys, L., De Proft, F., Weckhuysen, B.M., Van Speybroeck, V.: Mechanistic characterization of zeolite-catalyzed aromatic electrophilic substitution at realistic operating conditions. JACS Au. **2**, 502–514 (2022)

59. (a) Hernandez, E.D., Jentoft, F.C.: Spectroscopic signatures reveal cyclopentenyl cation contributions in methanol-to-olefins catalysis. *ACS Catal*. **10**, 5764–5782 (2020); (b) Wulfers, M. J., Jentoft, F. C.,

The role of cyclopentadienium ions in methanol-to-hydrocarbons chemistry. *ACS Catal.* 4, 3521–3532 (2014); (c) Srinivasan, P.D., Zhu, H., Bravo-Suárez, J.J.: *In situ* UV-Vis plasmon resonance spectroscopic assessment of oxygen and hydrogen adsorption location on supported gold catalysts. Mol. Catal. **507**, 111572 (2021); (d) Ishida, R., Hayashi, S., Yamazoe, S., Kato, K., Tsukuda, T.: Hydrogen-mediated electron doping of gold clusters as revealed by *in situ* X-ray and UV-Vis absorption spectroscopy. J. Phys. Chem. Lett. **8**, 2368–2372 (2017)

60. Grabow, K., Bentrup, U.: Homogeneous catalytic processes monitored by combined in situ ATR-IR, UV-Vis, and Raman spectroscopy. ACS Catal. **4**, 2153–2164 (2014)

61. Tromp, M., van Strijdonck, G.P.F., van Berkel, S.S., van den Hoogenband, A., Feiters, M.C., de Bruin, B., Fiddy, S.G., van der Eerden, A.M.J., van Bokhoven, J.A., van Leeuwen, P.W.N.N., Koningsberger, D.C., van Koten, G.: Organometallics. **29**, 3085–3097 (2010); (a) Tromp, M., Sietsma, J.R.A., van Bokhoven, J.A., van Strijdonck, G.P.F., van Haaren, R.J., van der Eerden, A.M.J., van Leeuwen, P.W.N.M., Koningsberger, D.C.: Chem. Commun. **128-129** (2003); (b) Bartlett, S.A., Wells, P.P., Nachtegaal, M., Dent, A.J., Cibin, G., Reid, G., Evans, J., Tromp, M.: J. Catal. **284**, 247–258 (2011)

62. Grauke, R., et al.: Impact of Al activators on structure and catalytic performance of Cr catalysts in homogeneous ethylene oligomerization – a multitechnique in situ/operando study. ChemCatChem. **12**, 1025–1035 (2019)

63. (a) Wijten, J.H.J., et al.: Electrolyte effects on the stability of Ni−Mo cathodes for the hydrogen evolution reaction. ChemSusChem. **12**, 3491–3500 (2019); (b) Wijten, J.H.J., Mandemaker, L.D.B., van Eeden, T.C., Dubbeld, J.E., Weckhuysen, B.M.: In situ study on Ni–Mo stability in a water-splitting device: effect of catalyst substrate and electric potential. ChemSusChem. **13**, 3172–3179 (2020)

64. Wahl, S., et al.: *Operando* diffuse reflectance UV-Vis spectroelectrochemistry for investigating oxygen evolution electrocatalysts. Catal. Sci. Technol. **10**, 517–528 (2020)

65. Segerer, A., Nitschke, P., Gschwind, R.M.: Combined in situ illumination-NMR-UV/Vis spectroscopy: a new mechanistic tool in photochemistry. Angew. Chem. Int. Ed. **57**, 7493–7497 (2018)

66. Valencia, S., Marín, J.M., Restrepo, G., Frimmel, F.H.: Application of excitation-emission fluorescence matrices and UV/Vis absorption to monitoring the photocatalytic degradation of commercial humic acid. Sci. Total Environ. **442**, 207–214 (2013)

67. Vogt, C., Weckhuysen, B.M.: The concept of active sites in heterogeneous catalysis. Nat. Rev. Chem. **6**, 89–111 (2022)

Charlotte Vogt received her Ph.D. with highest distinctions from Utrecht University in 2020 working with professor Bert Weckhuysen. In 2021, she was named one of "Forbes 30 under 30 Europe" and started her own research group as assistant professor at the Technion Institute for Technology in Israel, which focuses on a deep fundamental understanding of catalytic processes.

Caterina Suzanna Wondergem received her Ph.D. from Utrecht University, The Netherlands, in 2019. During this time, she worked on the development of *in situ* techniques for heterogeneous catalysis with professor Bert Weckhuysen. In 2020, she received a JSPS postdoctoral fellowship from the Japanese Society for the Promotion of Science to work on advanced X-ray imaging of electrocatalysts at Nagoya University.

Bert Weckhuysen is Distinguished University Professor at Utrecht University. His group focuses on the development of *in situ* and operando spectroscopy and microscopy to investigate solid catalysts at work. For his work, he has received national and international awards, including the International Catalysis Award and the Spinoza Prize. He is an elected (foreign) member of a.o. KNAW, KVAB and Academia Europeae.